Strong Uranium(VI) Binding onto Bovine Milk Proteins, Selected Protein Sequences and Model Peptides

Zänker, H.; Heine, K.; Weiss, S.; Brendler, V.; Husar, R.; Bernhard, G.; Gloe, K.; Henle, T.; Barkleit, A.;

Originally published:

March 2019

Inorganic Chemistry 58(2019), 4173-4189

DOI: https://doi.org/10.1021/acs.inorgchem.8b03231

Strong Uranium(VI) Binding onto Bovine Milk Proteins, Selected Protein Sequences and Model peptides

Harald Zänker,[a] Katja Heine,[a,b,#] Stephan Weiss,[a] Vinzenz Brendler,[a] Richard Husar,[a] Gert Bernhard,[a] Karsten Gloe,[b] Thomas Henle,[b] Astrid Barkleit[a,*]

[a] Helmholtz-Zentrum Dresden - Rossendorf, Institute of Resource Ecology, Bautzner Landstraße 400, 01328 Dresden, Germany

[b] Technische Universität Dresden, Faculty of Chemistry and Food Chemistry, 01062 Dresden, Germany

Present address: Berliner Glas, Waldkraiburger Straße 5, 12347 Berlin, Germany

* Corresponding author. E-Mail: a.barkleit@hzdr.de

Abstract

Hexavalent uranium is ubiquitous in the environment. In view of the chemical and radiochemical toxicity of uranium(VI) a good knowledge of its possible interactions in the environment is crucial. The aim of this work was to identify typical binding and sorption characteristics of uranium(VI) with both the pure bovine milk protein β-casein and diverse related protein mixtures (caseins, whey proteins). For comparison selected model peptides representing the amino acid sequence 13-16 of β-casein and dephosphorylated β-casein were also studied. Complexation studies using potentiometric titration and time-resolved laser-induced fluorescence spectroscopy revealed that the phosphoryl-containing proteins form uranium(VI) complexes of higher stability than the structure-analog phosphoryl-free proteins. That is in agreement with the sorption experiments showing a significantly higher affinity of caseins towards uranium(VI) in comparison to whey proteins. On the other hand, the total sorption capacity of caseins is lower than that of whey proteins. The discussed binding behavior of milk proteins to uranium(VI) might open up interesting perspectives for sustainable techniques of uranium(VI) removal from aqueous solutions. That was further demonstrated by batch experiments on the removal of uranium(VI) from mineral water samples.

Introduction

Uranium, an element of both chemotoxicity and radiotoxicity, is ubiquitous in the environment. Ground waters and surface waters contain traces of uranium which arise from natural and anthropogenic uranium sources.[1-3] A limit of 30 $\mu g\,L^{-1}$ uranium was recommended for drinking water by the World Health Organization (WHO).[4-6] In the majority of cases worldwide this limit value is well met or clearly undercut. However, there are also cases where the limit is exceeded or where there are concerns that it might become exceeded in the future. This includes both tap drinking water[2-5] and bottled mineral water.[7] High uranium concentrations in natural waters are due to the weathering of uranium-containing minerals[3] as well as anthropogenic influences such as mining activities,[1-3] the excessive use of phosphate fertilizers,[3, 8, 9] the use of uranium-containing ammunition,[10, 11] or nuclear accidents.[12, 13]

In aerobic systems, uranium exists mainly in the hexavalent state as the uranyl cation, UO_2^{2+}, which renders it relatively soluble in natural waters and, thus, relatively mobile in the environment. The uranyl ion is a Lewis acid metal ion with a trans-oxo group being formally trifold, having an effective charge of +3.2[14] and thus constituting a strong acid within the HSAB concept.[15] It forms stable complexes only in the equatorial plane and namely with Lewis bases such as hydroxide, carbonate or phosphate.[16-18] This includes reactions with organic ligands possessing strong binding functions such as carboxyl, hydroxyl, amino or phosphoryl groups.[18-20] These groups are abundant in peptides and proteins; their multifaceted reactions with the uranyl ion are discussed in the literature to an increasing extent.[21-28] Especially phosphoryl-containing proteins with strong binding properties for heavy metal ions including the uranyl ion are in the focus of interest.[29-35]

Uranium finds its way into the human body via potable water and fresh plants such as vegetables and fruits, but also via the detour of animal products.[3, 36] Although the consumption of milk is normally not the primary pathway of uranium incorporation by

humans, the relatively high proportion of milk and dairy products in the human diet and the complex composition of milk make the investigation of uranium interactions with the constituents of milk an essential task. Milk and dairy products are an important link in the food chain of humans. In particular, a high fraction of baby food is based on milk and milk products. The uranium concentration of bovine milk is typically <1 μg L^{-1} (<$4 \cdot 10^{-9}$ M),[36, 37] even though higher concentrations have also been reported.[38] Milk is a very complex system consisting of a multitude of components, among them especially proteins of different structure and bioactivity.[39, 40] Figure S1 (Supporting Information) gives a schematic illustration of the composition of cow milk. The two major protein groups in bovine milk are caseins (80%) and whey proteins (20%).[41] The main difference between the two groups is the presence of strong binding phosphoryl functions in caseins. It is known, that different milk proteins bind a number of metal ions, especially transition metal ions, such as Mn^{2+}, Cu^{2+}, Zn^{2+}, Cd^{2+}, Hg^{2+}, Cr^{3+}, Fe^{3+}, but also the main group ions Mg^{2+}, Ca^{2+}, Pb^{2+}, Al^{3+} and In^{3+}.[42-45] Until now the knowledge about specific chemical interactions between UO_2^{2+} and the different milk components is very limited. To the best of our knowledge, there is only a paper by Bolisetty and Mezzenga[46] discussing the utilization of the whey protein β-lactoglobulin in the form of an amyloid-carbon hybrid membrane for binding and separation of uranyl ions from aqueous solutions.

The present study is aimed at investigating the reactions of uranium(VI) with milk proteins isolated from cow´s milk. A better knowledge of these reactions will improve our understanding of the behavior of uranium(VI) traces in the food chain. This may make the assessment of the damage to the human body in the case of uranium(VI) ingestion more reliable. Even though the principal mechanisms of uranium(VI) toxicity to humans are known there is still only insufficient knowledge about the molecular interactions underlying this toxicity.[1-3, 10, 11, 33-35] Improving this knowledge creates a base for the development of better decorporation strategies in the case of accidental uranium(VI) incorporation by individuals.[33-

[35] There is still a remarkable lack of efficient means for heavy metal decorporation.[47, 48] Biogenic remedies for uranium(VI) decorporation made from milk proteins which cause only few medical side effects are conceivable. Furthermore, milk proteins are also of interest from a technological point of view. A multitude of suggestions have been made to solve the problems of uranium(VI) removal from waters. This includes the purification of uranium(VI) containing mining or industrial waste waters, the removal of uranium(VI) traces from ground waters for obtaining potable water as well as the extraction of uranium(VI) from sea water for its use in energy production.[34, 46, 49-64] The sorbents suggested for uranium(VI) adsorption range from cost effective run-of-the-mill substances such as tannin,[61] chitin/chitosan[62] or algal/microbial/fungal biomass[63] to especially designed sophisticated protein scaffolds that are expected to act as tailor-made pockets for accommodating metal ions within their structures by chelation.[64] It needs to be elucidated if milk proteins or milk protein derivatives are suitable for uranium(VI) removal from environmental waters and if they may open up a new way of water purification being both efficient and cheap.

First, the interactions of uranium(VI) with selected bovine milk proteins have been investigated in our study using sorption experiments with uranium(VI) on isolated milk proteins. On the basis of the Langmuir isotherm, information on the loading capacity and the binding affinity of different milk proteins is derived. Second, the reaction between milk proteins and uranium(VI) is regarded as a complexation reaction of the uranyl ion with functional groups on the proteins and the complex stability constants for different milk proteins and different functional groups were determined. Third, the results gained from the reactions of uranium(VI) with the different milk proteins and the different functional groups are further specified by comparison with the results of uranium(VI) complexation experiments with synthetic low-molecular peptides (protein sequences) of structures similar to those of the natural milk proteins. Low-molecular peptides originating as fragments from milk proteins are also present in raw milk.[65] To identify the mechanisms of uranyl binding to milk proteins, the

reaction of uranium(VI) with β-casein was compared with the reaction with less complex synthetic peptides representing the amino acid sequence 13-16 of β-casein (Val-Glu-Ser^{P}-Leu; VES^{P}L; explanation of the abbreviations see Scheme 1). Moreover, this sequence was also modified. To assess the influence of the steric properties of the N-terminal amino acid, Val was substituted by Gly (GES^{P}L). To prevent any influence of the β-carboxyl group of Glu, this amino acid was substituted in VES^{P}L by Ala (VAS^{P}L). The peptides were also synthesized as their unphosphorylized versions to investigate the uranyl complexation in the absence of phosphoryl groups (VESL, GESL and VASL). Furthermore, Ser in VESL was substituted by Ala to find out if the ß-hydroxy group of Ser is involved in uranyl binding (VEAL). Scheme 1 shows the chemical structure of the synthetic peptides. The tetrapeptides were not protected at their termini. Consequently, some carboxylic acid and amine functions are available for uranyl binding that are not accessible in the same fragment of the protein. Nevertheless, investigating the influence of the phosphoryl groups as the most important focus of this study was possible. Finally, the results received for caseins were also compared with those of uranyl complexation experiments employing dephosphorylated casein.

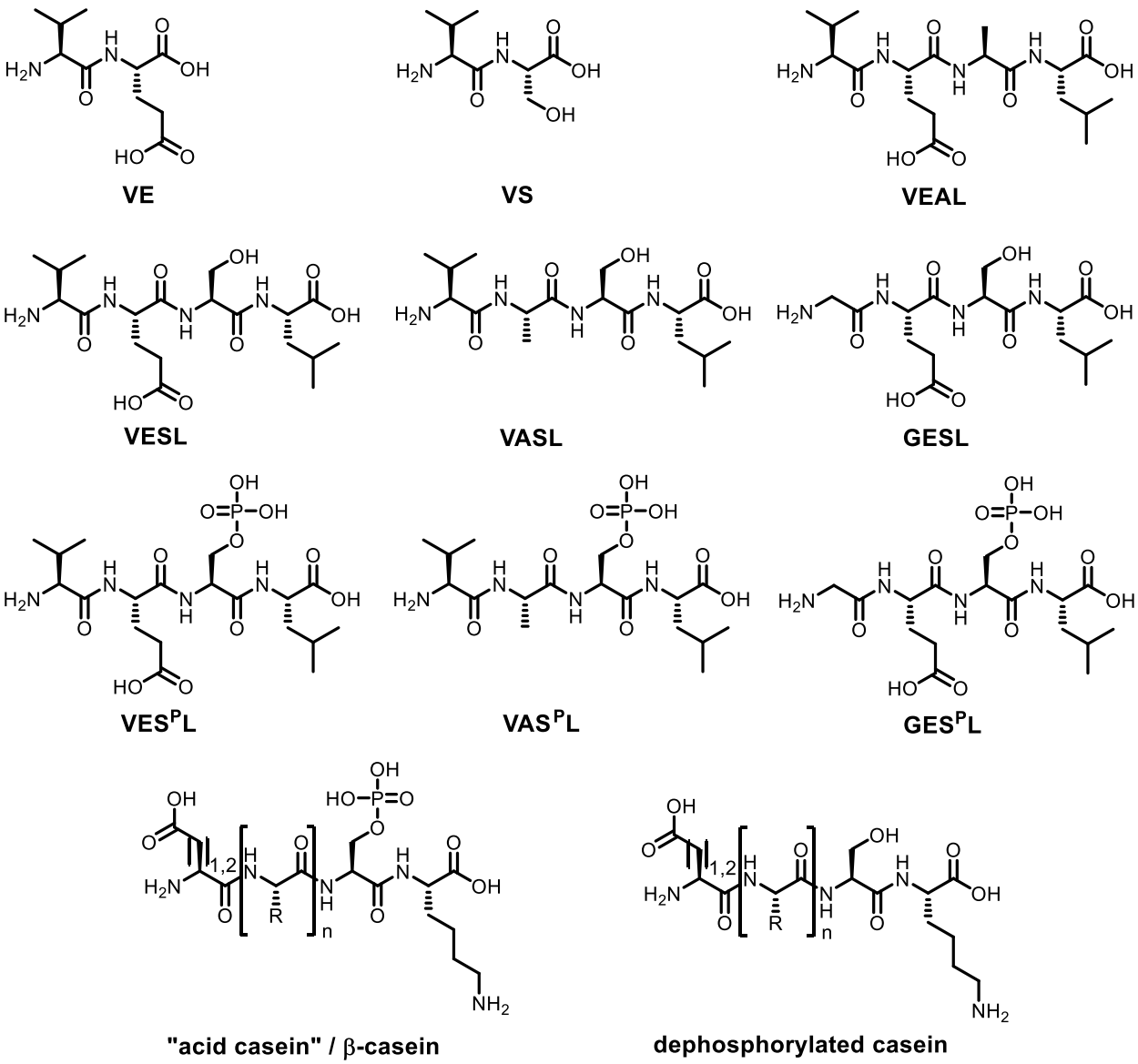

Scheme 1. Structure of the synthetic model ligands L-Valinyl-L-glutamic acid (VE), L-Valinyl-L-serine (VS), L-Valinyl-L-glutamyl-L-alanyl-L-leucin (VEAL), L-Valinyl-L-glutamyl-L-seryl-L-leucin (VESL), L-Valinyl-L-alanyl-L-seryl-L-leucin (VASL), Glycyl-L-glutamyl-L-seryl-L-leucin (GESL), L-Valinyl-L-glutamyl-L-phosphoseryl-L-leucin (VES^{P}L), L-Valinyl-L-alanyl-L-phosphoseryl-L-leucin (VAS^{P}L), Glycyl-L-glutamyl-L-phosphoseryl-L-leucin (GES^{P}L) and the proteins casein and dephosphorylated casein.

Results and discussion

Adsorption of uranium(VI) onto milk proteins

Screening experiment. Table 1 gives the distribution of uranium(VI) in the three fractions of our screening experiment with undiluted skim milk at pH 4.6 and 6.7. The screening experiment qualitatively illustrates the high sorption affinity of milk proteins for uranium(VI). More than 99% of the uranium(VI) is removed by the milk proteins (casein and whey) from the samples; uranium(VI) is not even detectable in most of the 10-kD ultra filtrates, i.e., the removal of the uranium(VI) is almost complete.

Table 1. Distribution of uranium(VI) in undiluted pasteurized and homogenized skim milk (screening experiment at varied pH).

pH	Adjusted uranium concentration [M]	Fraction of uranium [%] Pellet (mostly casein)	Centrifugate (whey)	10-kD filtrate of whey
4.6	10^{-5}	99.9	0.06	≤ 0.1
	10^{-6}	99.7	0.4	≤ 0.1
	10^{-7}	86	14.4	≤ 0.1
6.7	10^{-5}	92.8	7.0	0.2
	10^{-6}	94	6.0	≤ 0.1
	10^{-7}	99.9	≤ 0.1	≤ 0.1

Adsorption of uranium(VI) onto the unseparated milk protein fraction. Figure 1 a shows the adsorption isotherm of uranium(VI) onto the unseparated milk protein fraction of >10 kDa at pH 4.6. The starting point of assessing sorption data should be a physical model of the sorption process. The caseins form micelles cross-linked by colloidal calcium phosphate which are tens to hundreds of nm in size[41, 66] and even the constituents of such casein micelles, the casein macromolecules, have molecular weights of many thousands of Daltons.[41] Whey proteins, too, have molecular weights of thousands of Daltons.[67] This means that the milk protein particles are much bigger than the uranyl ions or inorganic uranyl complexes in the water. Because of this difference we classify the reaction between uranyl and the milk

proteins as adsorption in this part of our study. We regard our system as a two-phase system with the crucial interaction occurring at the protein-water interface (also considering that this system is easily converted from a “microscopic” two-phase system into a “macroscopic” two-phase system as for instance by ultracentrifugation or by casein precipitation with an acid). A reasonable approach of describing such a system is the application of a surface complexation model since it is plausible that the adsorption reaction proceeds at specific sites, i.e., functional groups (see also following paragraphs). However, for one specific (constant) pH value, as in our case, there is no difference between a surface complex formation constant and a Langmuir adsorption constant, K_L.[68] Therefore, we apply the Langmuir model in this part of the study and fit our experimental adsorption isotherm (Figure 1 a) to a Langmuir isotherm which has the form

$$Q = Q_{max} \frac{K_L \, c_{eq}}{1 + K_L \, c_{eq}} \qquad (1)$$

where Q (mol g^{-1}) is the amount of uranium(VI) adsorption, Q_{max} (mol g^{-1}) is the maximum amount of uranium(VI) adsorption (adsorption capacity), and K_L (L mol^{-1}) is the Langmuir isotherm constant. The fit provides a reasonable result for uranium(VI) equilibrium concentrations of up to 0.3 mg L^{-1} ($1.3 \cdot 10^{-6}$ M). Both, the high sorption affinity (K_L is a measure of the sorption affinity) and the high sorption capacity, Q_{max}, of the milk proteins for uranium(VI) are reflected in the fit. Table 2 gives the fit parameters together with the coefficient of determination, R^2, of the fit and the standard errors of the individual fit parameters.

.

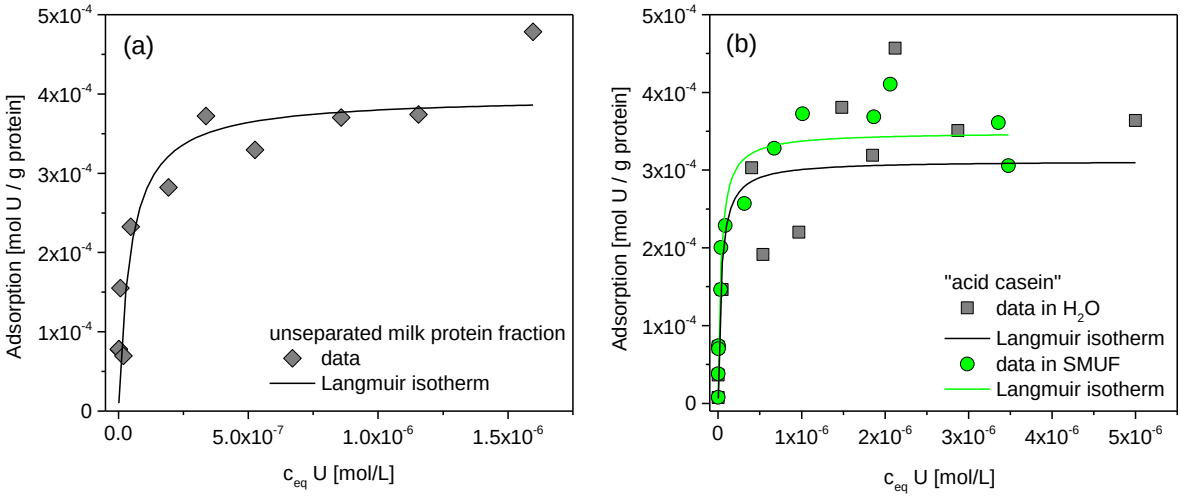

Figure 1. Experimental data and fitted Langmuir isotherm of uranium(VI) adsorption at pH 4.6 onto the unseparated milk protein fraction of >10 kDa (obtained from pasteurized and homogenized milk) (a) and "acid casein" (obtained from fresh milk) in water (black) and in SMUF solution (green) (b).

Table 2. Parameters of uranium(VI) adsorption onto "acid casein", whey proteins in water and SMUF and the unseparated milk protein fraction >10 kDa based on the Langmuir isotherm (pH 4.6). Tentative values are given in italics.

Langmuir parameter	"Acid casein"		Whey protein		Unseparated milk protein fraction
	H_2O	SMUF	H_2O	SMUF	
Q_{max}	$3.1 \cdot 10^{-4}$	$3.5 \cdot 10^{-4}$	*$1.2 \cdot 10^{-3}$*	*$8.0 \cdot 10^{-4}$*	$4.0 \cdot 10^{-4}$
[mol U(g protein)$^{-1}$]	($\pm 0.3 \cdot 10^{-4}$)	($\pm 0.2 \cdot 10^{-4}$)	*($\pm 0.1 \cdot 10^{-3}$)*	*($\pm 2.3 \cdot 10^{-4}$)*	($\pm 0.5 \cdot 10^{-4}$)
K_L	$2.7 \cdot 10^{7}$	$2.9 \cdot 10^{7}$	*$4.7 \cdot 10^{6}$*	*$2.0 \cdot 10^{5}$*	$2.0 \cdot 10^{7}$
[L(mol U)$^{-1}$]	($\pm 1.7 \cdot 10^{7}$)	($\pm 0.6 \cdot 10^{7}$)	*($\pm 1.4 \cdot 10^{6}$)*	*($\pm 1.0 \cdot 10^{5}$)*	($\pm 1.0 \cdot 10^{7}$)
R^2	0.90	0.97	*0.86*	*0.84*	0.72

Adsorption of uranium(VI) onto the separated casein and whey protein fractions. Figure 1 b shows isotherms of uranium(VI) adsorption onto casein separated from fresh milk ("acid casein"). The data were fit to the Langmuir isotherm and both, the adsorption capacity, Q_{max}, and the Langmuir adsorption constant, K_L, were derived as described above. The similarity of the isotherms in Figure 1 a and b is obvious. It demonstrates that, at least in the concentration range covered by Figure 1 a and b, the adsorption behavior of milk proteins is governed by the adsorption of uranium(VI) onto the caseins. This can also be seen from the adsorption parameters Q_{max} and K_L given in Table 2 that are very similar for the "acid casein" and the unseparated milk protein fraction. Another important finding is that the casein experiments in

water and in the phosphate-containing SMUF yield very similar results indicating that the affinity of casein to uranium(VI) is even higher than the affinity of inorganic phosphate to uranium(VI).

Uranium(VI) adsorption experiments were also performed on the whey protein fraction separated from fresh milk. The results are given in Figure S2, Supporting Information. Three pieces of information are obvious from Figure 1 and Figure S2, Supporting Information:

(i) The slope of the isotherms in the origin of co-ordinates, i.e., the sorption affinity, is much lower for the whey proteins than for the caseins.

(ii) Whey proteins can reach a higher sorption loading (may possess a higher sorption capacity) than caseins.

(iii) There is a large difference in the experiments of whey proteins between water and SMUF (the inorganic phosphate can outcompete the whey protein in uranium(VI) complexation which is not possible for caseins and which emphasizes the higher uranyl affinities of caseins in comparison with whey proteins).

Unfortunately, the results showed broad scattering of data in the case of whey proteins. The reasons for this scattering are not clear. It may have been caused by technical problems since we found significant residues of inorganic phosphate in our samples resulting from the protein separation process. Phosphate is able to compete with uranyl adsorption onto the organic ligands in the case of whey proteins whereas it is not in the case of caseins (see above). However, there may also be intrinsic reasons because caseins have a random coil structure whereas whey proteins possess a tertiary structure[69] which may hamper the access of uranyl to the binding sites of whey proteins as long as the tertiary structure is not unfolded. We do not have information about the folding states of the whey proteins under the conditions of our experiments. Nevertheless, we also derived values of Q_{max} and K_L for the whey proteins. We give them in italics only in Table 2; they should be taken as "tentative" values because of the strong scatter in data. The values of Q_{max} in Table 2, too, suggest that whey proteins possess a

significantly higher adsorption capacity for uranium(VI) ($1.2 \cdot 10^{-3}$ mol g^{-1} in H_2O and $8.0 \cdot 10^{-4}$ mol g^{-1} in SMUF) than the caseins ($3.1 \cdot 10^{-4}$ mol g^{-1} in H_2O and $3.5 \cdot 10^{-4}$ mol g^{-1} in SMUF), but that the Langmuir constant K_L in H_2O and SMUF is much lower for the whey proteins than for the caseins ($4.7 \cdot 10^6$ and $2.0 \cdot 10^5$ L mol^{-1} instead of $2.7 \cdot 10^7$ and $2.9 \cdot 10^7$ L mol^{-1}). In particular the difference in K_L (indicating sorption affinity) is striking. In the following sections we show that this is due to the presence of phosphoserine (P-Ser) residues in the structure of the caseins which whey proteins do not possess. Table S1 (Supporting Information) gives the number of phosphoryl groups per molecule for the individual caseins.

A link between the uranyl loading capacity Q_{max} and the chemical composition of the casein can be established. A loading capacity of $3.1 \cdot 10^{-4}$ mol g^{-1} was found for "acid casein" in H_2O (Table 2). From the molecular weights of the individual casein components and the percentage composition of bovine casein (Table S1, Supporting Information) an "average molecular weight" of the "acid casein" can be derived. It amounts to 22.4 kDa. We can conclude from this value that the maximum loading of our "acid casein" is about 7 mol uranium(VI) per mol casein. From the number of the P-Ser residues of the individual caseins (Table S1, Supporting Information) and the percentage composition of the casein mixture an "average number" of phosphoryl groups in the molecules of "acid casein" of ~6 can be derived. Considering the uncertainty of the measured value of Q_{max} and that carboxylic groups start to play a role in addition to the phosphoryl groups when the uranyl-phosphoryl complexation approaches saturation (see following paragraphs), a slightly higher uranium(VI) loading of 7 mol uranium(VI) per mol casein than that to be expected from the number of phosphoryl moieties in the casein mixture alone, i.e. 6 mol uranium(VI) per mol casein, is a reasonable approximation.

Sorption experiments with uranium-rich natural spring water. The adsorption power of casein was also demonstrated by sorption experiments with uranium-rich natural spring water (Heinrichsquelle Nürtingen). We found a uranium concentration of 371 µg L^{-1} ($1.56 \cdot 10^{-6}$ M)

in this water. In the as-received state of the water (pH 8.3), 97.2% of the uranium was able to pass through a 10-kDa filter and was found in the ultra-filtrate, i.e., could be regarded as existing in a truly dissolved form such as uranyl carbonato or calcium uranyl carbonato complexes.[70] The picture changes if "acid casein" is added to the spring water (pH 8.3). Only 3.2% of the uranium is still able to pass through the filters under this condition. Most of the uranium (96.8%) is removed from the truly dissolved fraction and bound to the casein. After acidification to pH 4.6 the removal and binding to the casein was virtually complete; less than 0.15% of the uranium passed through the ultrafilter (see Figure 2). The experiment shows that casein is an effective adsorbens for uranium, even if the pH is increased and the carbonate concentration is high (compared to that of groundwater, drinking water etc.).

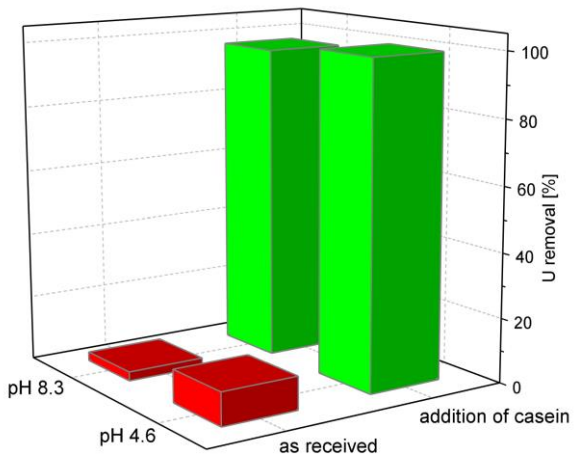

Figure 2. Removal of uranium from uranium-rich natural spring water by ultrafiltration with and without addition of β-casein at different pH.

Deprotonation behavior of the peptides and proteins

The potentiometric titration curves of the pure ligands in the absence of uranium(VI)[71] were analyzed based on the deprotonation of discrete monoprotic acids according to reaction

$$R{-}A_iH \leftrightarrows R{-}A_i^- + H^+ \qquad (2)$$

where R is the ligand with the functional groups A_i. The corresponding deprotonation constant K_a can be written as

$$K_a = \frac{[R - A_i^-][H^+]}{[R-A_iH]} \quad (3)$$

$[R-A_i^-]$ and $[R-A_iH]$ represent the concentrations of the deprotonated and protonated forms of the functional group A_i and $[H^+]$ is the proton concentration in the solution. The ligands investigated include carboxyl, phosphoryl, amino and hydroxyl groups. Table 3 shows potential deprotonation reactions together with the pK_a ranges to be expected for these groups in peptides and proteins.[72-75]

Table 3. Potential deprotonation reactions and pK_a ranges to be expected for the corresponding functional groups in peptides and proteins.[72-75]

Functionality	Dissociation equation	pK_a range
α-COOH	R-COOH ⇄ R-COO$^-$	2.3 – 3.3
β,γ-COOH		3.2 – 4.8
-OPO_3H_2	R–O–PO_3H_2 ⇄ R–O–PO_3H^- + H^+	0.5 – 1.0
-OPO_3H^-	R–O–PO_3H^- ⇄ R–O–PO_3^{2-} + H^+	5.5 – 6.2
α-NH_3^+	R-NH_3^+ ⇄ R-NH_2 + H^+	7.4 – 9.1
ε-NH_3^+		9.9 – 11.1
-OH	R-OH ⇄ R-O$^-$ + H^+	9.9 – 12.5

To provide a base for the interpretation of the protonation and binding behavior of β-casein, selected synthetic di- and tetrapeptides were included in the study. The peptides represent the protein sequence 13-16 of β-casein. Further modifications were performed to test whether or not different functionalities cause differences in the protonation and complexation behavior (see Introduction and Scheme 1). The fit of the experimental data was done with the HYPERQUAD code.[76]

Table 4 gives the stepwise deprotonation constants pK_a derived from the titration curves. The titration curves together with the fits and the resulting speciation diagrams of the systems

(species concentration *vs.* pH) together with the chemical structure of the involved species can be found in Figures S3 through S10 (Supporting Information).

Table 4. Stepwise deprotonation constants of the peptides and proteins determined by potentiometric titration at T = 25 °C and I = 0.1 M ($NaClO_4$).

	pK_a[a]					
	-OPO_3H_2	α-COOH	β,γ-COOH	-OPO_3H^-	α-NH_3^+	ε-NH_3^+/-OH
VE		3.16(1)	4.42(1)		8.09(1)	
VE[b]		3.15(1)	4.36(1)		8.05(1)	
VS		3.18(1)			7.86(1)	
VESL		3.54(1)	4.22(1)		7.90(1)	
VASL		3.42(1)			7.65(2)	
GESL		3.19(1)	4.58(1)		8.16(1)	
VEAL		3.17(1)	4.39(1)		7.88(2)	
VES^PL	1.27(1)	3.57(1)	4.43(1)	6.45(1)	8.38(1)	
VAS^PL	1.12(2)	3.82(1)		6.27(2)	8.28(3)	
GES^PL	1.59(1)	3.63(1)	4.33(1)	6.08(1)	8.65(3)	
α-casein[c]	0.9	2.95	4.1	5.3	8.1	10.8
β-casein	1.51(1)	2.94(1)	4.61(1)	5.50(1)	7.11(1)	9.97(2)
"acid casein"	1.96(1)	3.05(1)	4.97(1)	5.50(1)	6.92(1)	9.92(2)
dephos. casein		2.99(1)	4.83(1)		6.34(1)	9.89(3)

[a] Errors of the last significant decimal place (σ) are given in parentheses.
[b] from Kallay et al.[77]; I = 0.2 M (KCl).
[c] from Österberg[72]; I = 0.15 M (KCl).

Good agreement of the deprotonation constants with the literature was found for the dipeptide VE.[77] On the basis of this information and of deprotonation constants for the amino acids Glu, Ser and P-Ser[71] (see Table S6, Supporting Information), conclusions on the more complex systems such as the tetrapeptides and the milk proteins can be drawn. That is, three deprotonation steps are expected and found for VE, i.e., that of the carboxyl group of the C-terminus, that of the carboxyl group of the Glu residue, and that of the amino group of the N-terminus. They are represented by the corresponding deprotonation constants in Table 4. Very similar constants are found for the tetrapeptides VESL/VES^PL, VEAL and GESL/GES^PL. Thus, the pK_a values of VE can be used for the identification of the deprotonation steps of these tetrapeptides. In Figure 3 the speciation diagram and the respective deprotonation steps of VESL are depicted as an example.

However, there are two more deprotonation steps in VES^{P}L and GES^{P}L compared to VE, VESL and GESL. This is due to the phosphorylation which introduces a new proton binding group showing two deprotonation steps. The speciation diagrams depicted in the Supporting Information (Figures S3, S6 and S7) reflect these differences in protonation behavior. Very similar diagrams are obtained for VE, VESL, VEAL and GESL (Figures S3 and S6, Supporting Information), but more species come into the play and more complex diagrams result for VES^{P}L and GES^{P}L (Figure S7, Supporting Information). The interpretation for VASL/VAS^{P}L is based on the dipeptide VS, missing the Glu residue (Table 4 and Figures S4, S6 b and S7 b, Supporting Information).

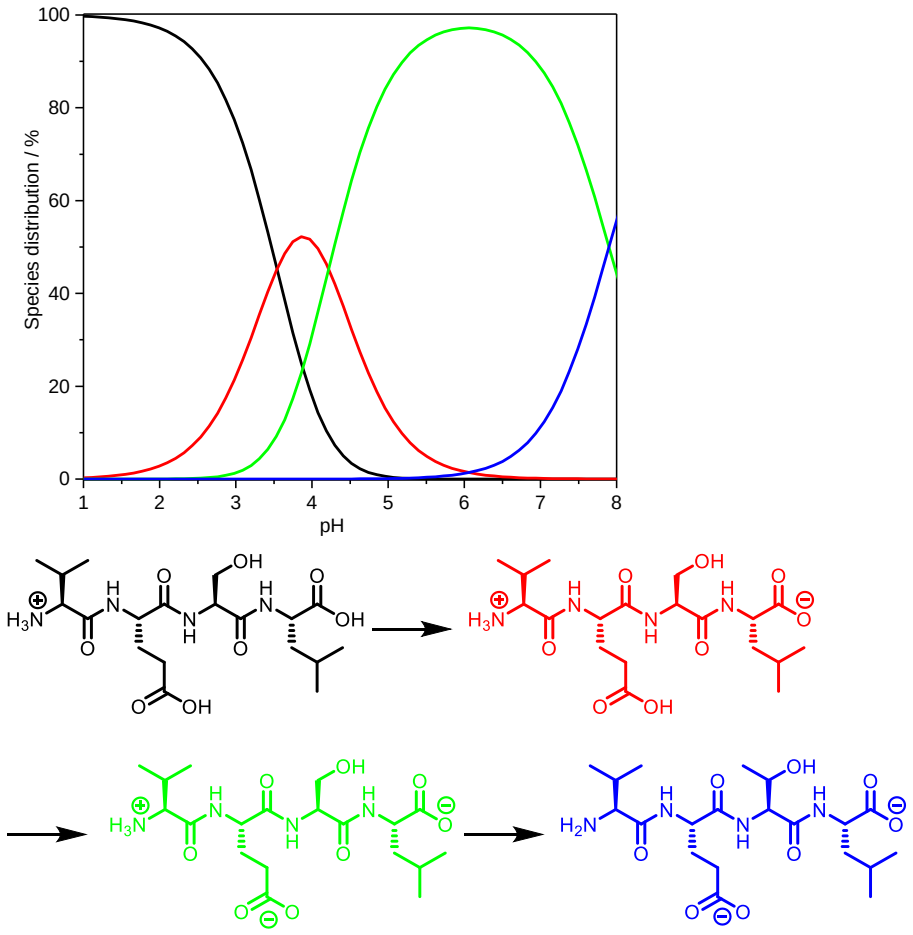

Figure 3. Speciation and respective species of the tetrapeptide VESL in dependence on pH at a peptide concentration of $3 \cdot 10^{-3}$ M (I = 0.1 M).

Six deprotonation constants could be identified for β-casein and "acid casein" (Table 4). On the basis of the results for the synthetic tetrapeptides these constants could be assigned as follows. The pK_a value of 2.94/3.05 refers to the carboxyl group of the C-terminus, the value of 7.11/6.92 relates to amino groups of the N-terminus of histidyl or cysteinyl residues and the values of 4.61/4.97 to carboxyl groups of aspartic acid (Asp) and Glu residues, whereas a value at 9.97/9.92 can be related to amino- or hydroxyl groups of lysyl, tyrosyl, or arginyl residues. The pK_a values of 1.51/1.96 as well as 5.50 refer to the phosphoryl groups of P-Ser residues. These pK_a values are within the range of the literature values published for α-casein (see Table 4).[72] The speciation diagrams of β-casein and "acid casein" (Figure S9, Supporting Information) bear resemblance to those of VES^{P}L and GES^{P}L (Figure S7, Supporting Information), except for the last dissociation step of the ε-NH_3- or OH-groups which are missing in the case of the tetrapeptides. Four proton binding constants were identified for the protein mixture obtained by alkaline dephosphorylation of "acid casein" (final degree of phosphorylation: 23%), belonging to carboxyl-, hydroxyl-, and amino groups (see Table 4). But although the casein was not completely dephosphorylated, no protonation constants belonging to these few remaining residual phosphoryl groups could be calculated. The effect of dephosphorylation is obvious. Figure S10 (Supporting Information) gives the corresponding speciation of dephosphorylated β-casein, resembling those of VESL and GESL (Figure S6, Supporting Information), except again for the last dissociation step of the ε-NH_3- or OH-groups which are missing in the case of the tetrapeptides.

The protonation constants determined for the proteins are apparent protonation constants. Since there is a multitude of protonable groups which cannot be distinguished from each other (e.g., differentiation between the individual Glu and Asp residues etc.), the protonation constants are obtained in the form of collective values. However, it is striking that the constants found for β-casein agree very well with those reported in the literature for the individual amino acids. This is likely due to the fact that the caseins mainly occur as open

chains in a random coil arrangement with no tertiary structure[69] which makes the functional groups well accessible.

Complex formation with uranium(VI) identified by pH potentiometry

The potentiometric titration data of the peptides and proteins in presence of the uranyl ion were analyzed based on the formal complex formation equation for discrete binding sites

$$x\ UO_2^{2+} + y\ R{-}A_i^{-} + z\ H^{+} \leftrightarrows [(UO_2)_x(R{-}A_i)_yH_z]^{x(2x-y+z)+} \quad (4)$$

and the mass action law which provides the complex stability constant log *K*:

$$K = \frac{[(UO_2)_x(R\text{-}A_i)_yH_z]}{[UO_2^{2+}]^x[R\text{-}A_i]^y[H^+]^z} \quad (5)$$

The pK_a values from the potentiometric ligand titrations (cf. Table 4) were used as initial data. The HYPERQUAD code[76] was used for the parameter derivation, including the uranyl hydrolysis constants taken from the respective NEA TDB volume (Table S7, Supporting Information).[18] These data are also the basis for all following speciation diagrams that include the uranyl cation.

Tables 5 and 6 give the stepwise complex stability constants of uranium(VI) with the di- and tetrapeptides VE, VS, VESL, VEAL, GESL, VASL, VES^{P}L, GES^{P}L and VAS^{P}L. Here it was assumed, that the respective complexations are highly reversible as they do not include any molecular re-structuring or changes in oxidation states and are occurring in homogeneous aqueous solution. Also other papers dealing with related reaction scenarios did not find any indications of irreversible complex formation.[33, 35, 77, 78] Moreover, the above assumption allows an overall interpretation that is free of internal contradictions.

Table 5. Stepwise stability constants of uranyl complexes with the synthetic dipeptides VE and VS determined by potentiometric titration at T = 25 °C and I = 0.1 M ($NaClO_4$).

VE			**VS**			deprotonation step
Species[a]	M L H[b]	log K[c]	Species[a]	M L H[b]	log K[c]	
$UO_2LH_2^{2+}$	1 1 2	4.11(4)				α-COO^-
UO_2LH^+	1 1 1	4.39(4)				γ-COO^-
$UO_2(LH)_2$	1 2 2	10.78(12)				γ-COO^-
UO_2L	1 1 0	7.43(6)	UO_2L^+	1 1 0	6.71(15)	α-NH_2
$UO_2L(OH)^-$	1 1 -1	-5.20(3)	$UO_2L(OH)$	1 1 -1	-4.82(7)	
$UO_2L(OH)_2^{2-}$	1 1 -2	-7.29(3)	$UO_2L(OH)_2^-$	1 1 -2	-6.37(9)	
			$UO_2L(OH)_3^{2-}$	1 1 -3	-8.39(18)	

[a] L stands for the completely deprotonated dipeptide; for the chemical formulas of the stepwise deprotonated ligand species see Figures S3 (VE) and S4 (VS), Supporting Information.
[b] M L H = metal/(completely deprotonated) ligand/H^+ (negative values stands for OH^-)
[c] Errors of the last significant decimal place (σ) are given in parentheses.

Table 6. Stepwise stability constants of uranyl complexes with the synthetic tetrapeptides determined by potentiometric titration at T = 25 °C and I = 0.1 M ($NaClO_4$).

Species[a]	M L H[b]	log K[c]			deprotonation step
		VESL	**GESL**	**VEAL**	
$UO_2LH_2^{2+}$	1 1 2		3.86(2)	4.11(3)	α-COO^-
UO_2LH^+	1 1 1	5.25(3)	5.01(2)	4.35(3)	γ-COO^-
UO_2L	1 1 0	6.59(7)	7.11(7)	7.04(3)	α-NH_2
$UO_2L(OH)^-$	1 1 -1	-4.72(3)	-4.93(3)	-5.44(3)	
$UO_2L(OH)_2^{2-}$	1 1 -2	-6.82(2)	-7.09(3)	-6.85(3)	
$UO_2L(OH)_3^{3-}$	1 1 -3	-8.56(3)	-9.15(15)	-9.11(16)	
		VASL			
UO_2L^+	1 1 0	6.26(11)			α-NH_2
$UO_2L(OH)$	1 1 -1	-4.66(5)			
$UO_2L(OH)_2^-$	1 1 -2	-6.30(4)			
$UO_2L(OH)_3^{2-}$	1 1 -3	-8.21(8)			
		VES^PL	**GES^PL**		
$UO_2LH_3^+$	1 1 3	2.49(1)	3.62(2)		α-COO^-
UO_2LH_2	1 1 2	5.03(1)	5.71(2)		γ-COO^-
UO_2LH^-	1 1 1	6.95(2)	7.13(2)		β-OPO_3^{2-}
UO_2L^{2-}	1 1 0	8.40(5)			α-NH_2
		VAS^PL			
$UO_2LH_2^+$	1 1 2	3.12(1)			α-COO^-
UO_2LH	1 1 1	6.44(2)			β-OPO_3^{2-}
UO_2L^-	1 1 0	9.02(4)			α-NH_2

[a] L stands for the completely deprotonated tetrapeptide; for the chemical formulas of the stepwise deprotonated ligand species see Figures 3 (VESL), S6 (GESL, VEAL, VASL) and S7 (VES^PL, GES^PL, VAS^PL), Supporting Information.
[b] M L H = metal/(completely deprotonated) ligand/H^+ (negative values stands for OH^-)
[c] Errors of the last significant decimal place (σ) are given in parentheses.

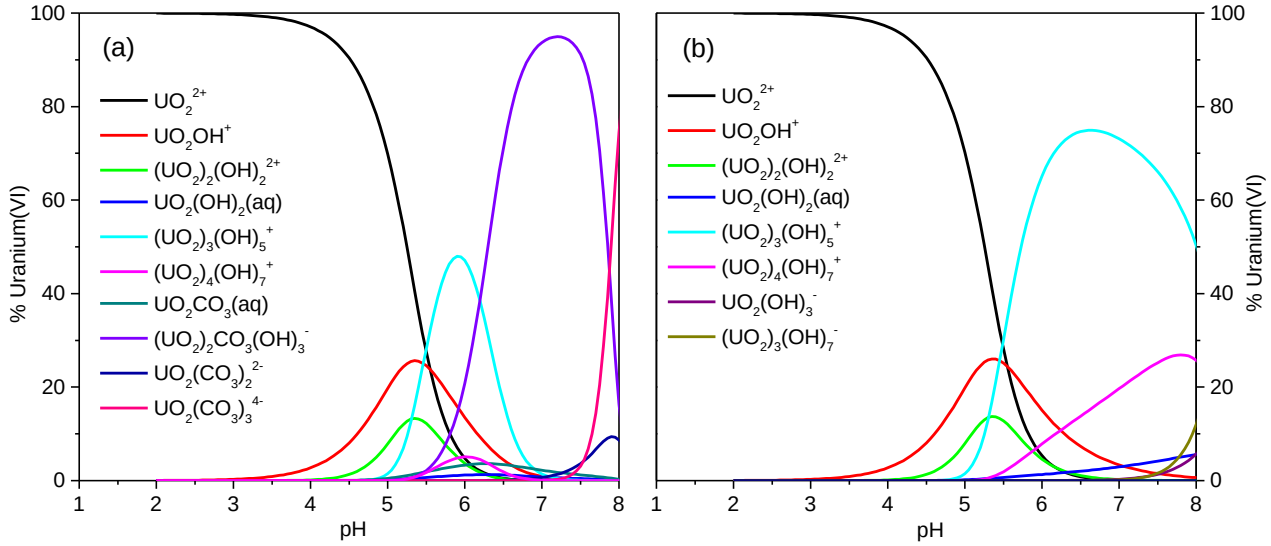

Figure 4. Speciation of uranium(VI) in dependence on pH at a uranyl concentration of $1.0 \cdot 10^{-5}$ M (I = 0.1 M $NaClO_4$) and under neglecting the formation of precipitates. Presence of CO_2 (p_{CO2} = $3.2 \cdot 10^{-4}$ bar) (a). Inert gas conditions (b).

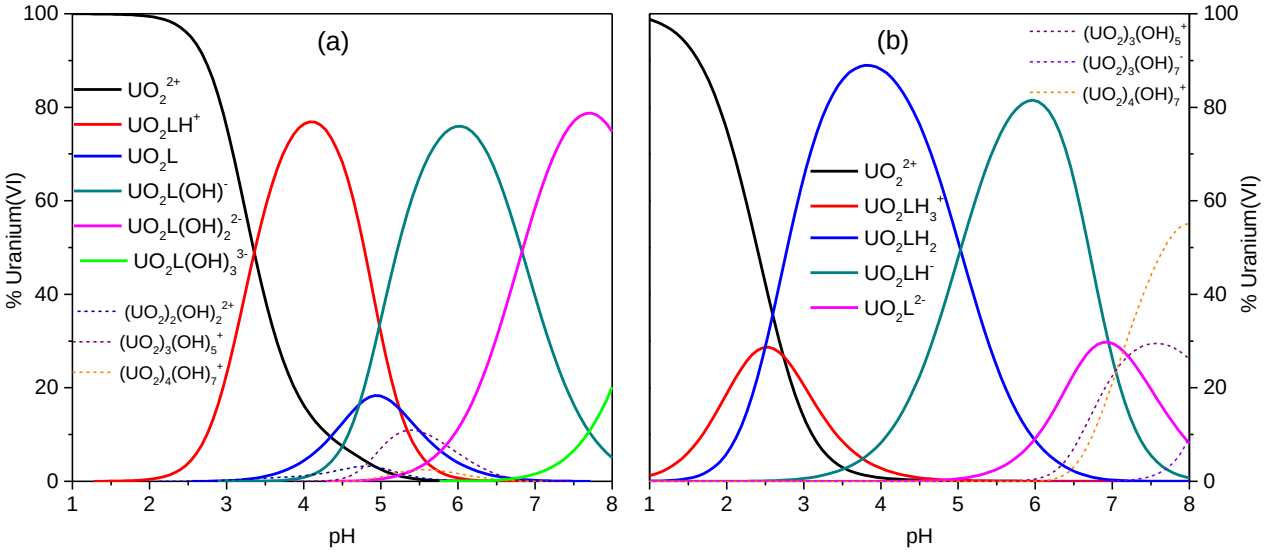

Figure 5. Speciation of uranium(VI) with VESL (a) and VES^{P}L (b) in dependence on pH at a uranyl concentration of $1.5 \cdot 10^{-3}$ M and peptide concentration of $3.0 \cdot 10^{-3}$ M (I = 0.1 M $NaClO_4$). Notation of the complexes can be found in Table 6.

In Figure 4 we show the speciation of uranium(VI), generated on the basis of the uranyl hydrolysis and uranyl carbonate constants (Table S7, Supporting Information) [18, 79] in water under ambient conditions (Figure 4 a) and under inert gas conditions, i.e., exclusion of CO_2 (Figure 4 b), as a reference. The speciation diagrams of uranium(VI) with VESL and

VES^PL,[80] based on the data from Table 6 and the uranyl hydrolysis constants (Table S7, Supporting Information),[18] can be found in Figure 5 as two examples. Further examples for the other peptides are shown in Figures S11 and S13 (Supporting Information). The uranium(VI) speciation in the presence of the peptides should be compared with Figure 4 b, because the experiments were carried out under inert gas conditions. For the tetrapeptides the results with respect to uranyl complexation can be generalized as follows:

(i) All tetrapeptides, whether or not possessing phosphoryl groups, suppress the formation of uranyl hydroxo complexes by forming their own strong complexes.

(ii) Tetrapeptides possessing phosphoryl groups cause stronger complexation in the acidic to neutral pH than those without phosphoryl groups.

(iii) Tetrapeptides without phosphoryl groups tend to form ternary uranyl hydroxo peptide complexes leading to a stronger complexation in the basic pH range compared to the complexes of phosphoryl containing tetrapeptides.

(iv) The modification of the tetrapeptide VESL with Gly (G) instead of Val (V), leading to GESL (without the t-butyl group of Val; see Scheme 1), results in the formation of stronger complexes, especially at very acidic pH.

(v) Substitution of Glu (E) in VESL with Ala (A), forming VASL (without the β-carboxyl group of Glu), causes weaker complexation in the acidic pH.

(vi) Replacing Ser (S) in VESL by Ala (A), resulting in VEAL (without the hydroxyl group of Ser), again, results in stronger complexation of UO_2^{2+} in the very acidic pH range.

(vii) For the phosphorylated tetrapeptides the effects (iv) through (vi) are less pronounced.

Consequently, the complexation behavior of the peptides is primarily dependent on the nature of the functional groups. This is especially pronounced at rather acidic pH values. However, effects caused by the structure of the whole ligand molecule (position of the functional groups within the structure, influences of the side chains in the vicinity of functional groups, chelate and scaffold effects etc.) are of less relevance.

Table 7 presents the stepwise stability constants of the uranyl complexes with β-casein, "acid casein" and dephosphorylated "acid casein" as determined by pH potentiometry. They can be related to the stability constants of the uranyl complexes with the peptide sequences (Tables 5 and 6) to identify the individual functional groups.

Table 7. Stepwise stability constants of uranyl complexes with β-casein, "acid casein" and dephosphorylated "acid casein" determined by potentiometric titration at T = 25 °C and I = 0.1 M ($NaClO_4$).

Species[a]	M L H[b]	log K[c]		deprotonation step
		β-casein	**"acid casein"**	
$UO_2LH_5^{3+}$	1 1 5	2.14(1)	1.69(2)	β-OPO_3H^-
$UO_2LH_4^{2+}$	1 1 4	2.48(3)	3.94(2)	α-COO^-
$UO_2LH_3^{+}$	1 1 3	4.57(5)	4.94(5)	β/γ-COO^-
UO_2LH_2	1 1 2	7.14(3)	7.29(3)	β-OPO_3^{2-}
UO_2LH^-	1 1 1	7.79(14)	7.97(11)	α-NH_2
UO_2L^{2-}	1 1 0	10.68(30)	10.86(24)	ε-NH_2
		dephosphorylated "acid casein"		
$UO_2LH_3^{3+}$	1 1 3	2.54(1)		α-COO^-
$UO_2LH_2^{2+}$	1 1 2	2.98(1)		β/γ-COO^-
UO_2LH^+	1 1 1	8.05(3)		α-NH_2
UO_2L	1 1 0	11.72(8)		ε-NH_2
$UO_2L(OH)^-$	1 1 -1	-6.78(3)		

[a] L stands for the completely deprotonated protein; chemical formulas of the stepwise deprotonated species see Figure S9 ("acid casein" and β-casein) and S10 (dephosphorylated "acid casein"), Supporting Information.
[b] M L H = metal/(completely deprotonated) ligand/H^+ (negative values stands for OH^-).
[c] Errors of the last significant decimal places (σ) are given in parentheses.

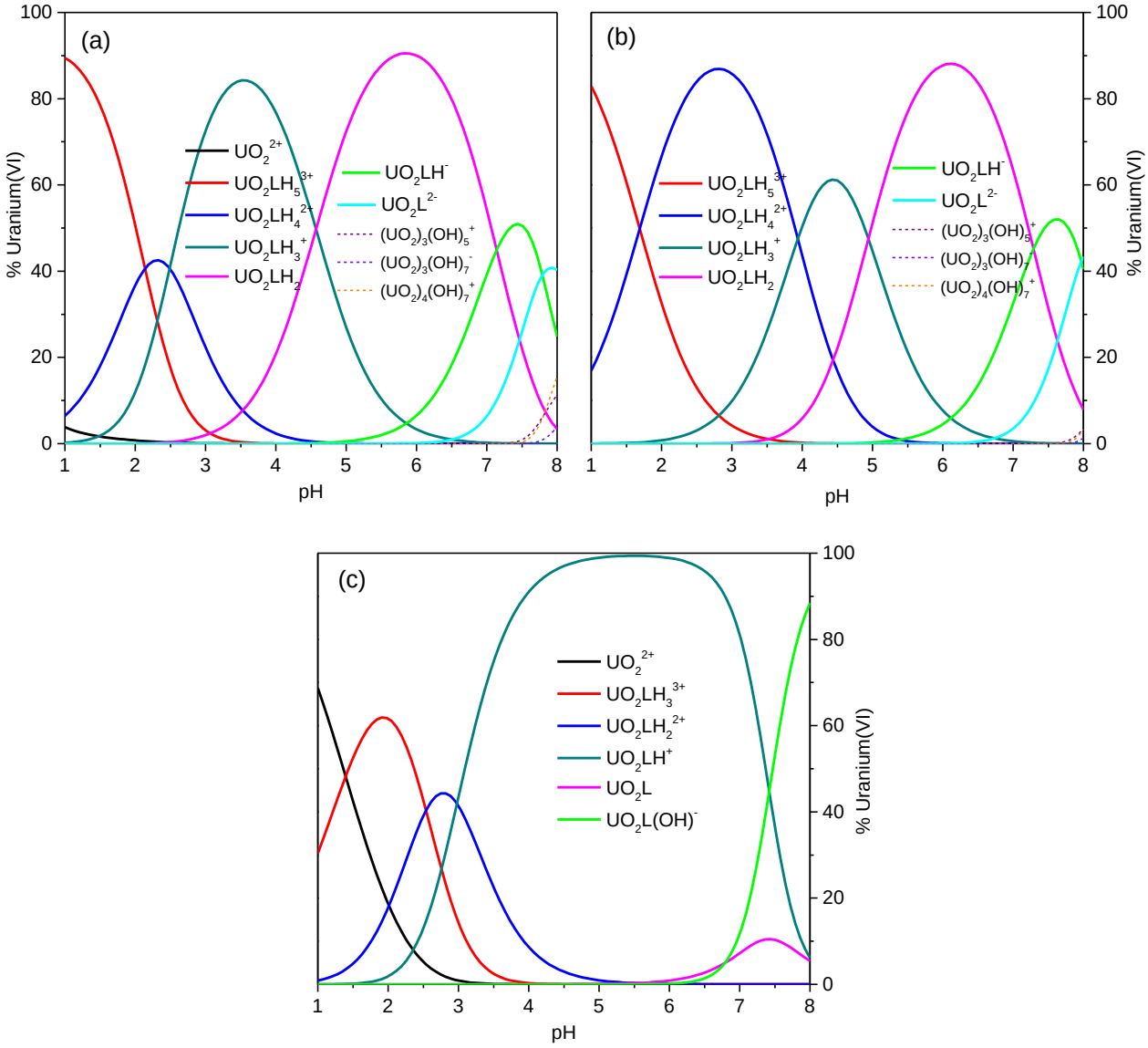

Figure 6. Speciation of uranium(VI) with ß-casein (a), "acid casein" (b) and dephosphorylated "acid casein" (c) in dependence on pH at a uranyl concentration of $1.0 \cdot 10^{-3}$ M and protein concentration of $3.0 \cdot 10^{-4}$ M (I = 0.1 M $NaClO_4$). Notation of the complexes can be found in Table 7.

The speciation diagrams[80] on the basis of the data from Table 7 and Table S7 (Supporting Information)[18] are depicted in Figure 6.

Six species were found for the complexation of UO_2^{2+} with β-casein. The speciation diagram (Figure 6 a) shows that the free uranyl ion is almost non-existent; at pH 1 already 90% of the uranium(VI) occurs as $UO_2LH_5^{3+}$. The main species at slightly less acidic pH is $UO_2LH_3^{+}$ and the dominating species at near-neutral pH of 4.5 to 7 is UO_2LH_2. At slightly alkaline pH UO_2LH^{-} and UO_2L^{2-} occur. Small amounts of binary uranyl hydroxo species appear only

above pH 7.5. Ternary species were not observed. Similar uranium(VI) complex species were also identified for the “acid casein”. As expected, their stability constants correlate relatively well with those of the β-casein, even though there are differences. The latter are also reflected in Figure 6 b which demonstrates that the complexation reactions in the two casein samples are similar but not identical.

Two species less than for β-casein and “acid casein” are expected for the complexation of the uranyl ion with dephosphorylated acid casein. We found five species which, however, include a ternary uranyl hydroxo species that did not appear with the phosphorylated casein forms. No complex stability constants corresponding to the phosphoryl group were found although 23% of the dephosphorylated “acid casein” was still phosphorylated. The missing of phosphoryl groups is also to be seen in the speciation diagram (Figure 6 c). In the strongly acidic region there is still free UO_2^{2+} before the species $UO_2LH_3^{3+}$ starts to dominate. The by far most prevailing species in the middle region of the pH scale is UO_2LH^+. In the alkaline region the ternary species $UO_2L(OH)^-$ appears. The results for the milk proteins fit into the picture obtained for the synthetic peptides and summarized in bullet points (i) through (vii) and support the conclusions drawn above.

However, the geometry and stability of the uranyl protein complexes is also influenced by structural features, such as steric effects or long-range interactions (e.g. electrostatic interactions, hydrogen bonding).[81] Possible unstructured domains and uncharacterized binding sequences within the protein scaffold could also have an influence.[27, 82-84] Thus, for instance, certain differences in uranium(VI) chelation behavior between caseins and whey proteins are to be expected because the former have a random coil conformation whereas the latter possess mainly α-helices and β-sheets.[69]

Complex formation with uranium(VI) characterized by TRLFS

Figure 7 shows the luminescence spectra of uranium(VI) in the presence of β-casein at a uranyl concentration of 10^{-5} M which is environmentally more representative than the concentrations of our pH potentiometric experiments. The β-casein concentration was $3.15 \cdot 10^{-5}$ M in the first test series (Figure 7 a) which corresponds to a uranyl / protein-function ratio of uranyl/carboxyl/phosphoryl = 1 : 75.1 : 15.6 (each β-casein molecule provides 24 carboxyl and 5 phosphoryl functionalities); the pH was varied between 2 and 7. For comparison, the spectrum of pure UO_2^{2+} at pH 1.91 is included. When adding the protein, a strong red shift of the peak maxima of about 10 nm occurs at pH 2.14 already, coupled with a strong increase of the luminescence intensity, indicating strong complex formation. In a second test series (Figure 7 b), the protein was successively added at a constant pH of 4.6, starting with a deficit of functional groups compared to UO_2^{2+} (uranyl/carboxyl/phosphoryl = 1 : 0.4 : 0.1 for 0.156 μM β-casein). The peak shift and the luminescence intensity rise are developing slowly and the peaks are broadening under the condition of uranyl excess. At a uranyl/phosphoryl ratio of approximately 1 : 1 (2.31 μM β-casein), the peaks become sharper, the red shift reaches its maximum and the further luminescence intensity increase becomes marginal. Because of the excess of carboxyl and the deficiency in phosphoryl groups prior to this point of equivalence, one can assume that mainly the carboxyl groups coordinate the uranyl ion below a phosphoryl/uranyl ratio of ~1 : 1, whereas phosphoryl coordination becomes prevailing at higher phosphoryl/uranyl ratios.

To verify this assumption, the synthetic tetrapeptides VESL, VASL, VES^{P}L and VAS^{P}L, which represent the protein sequence 13-16 of the β-casein, were complexed with uranium(VI) and investigated by TRLFS as a base for comparisons (Figure 8).

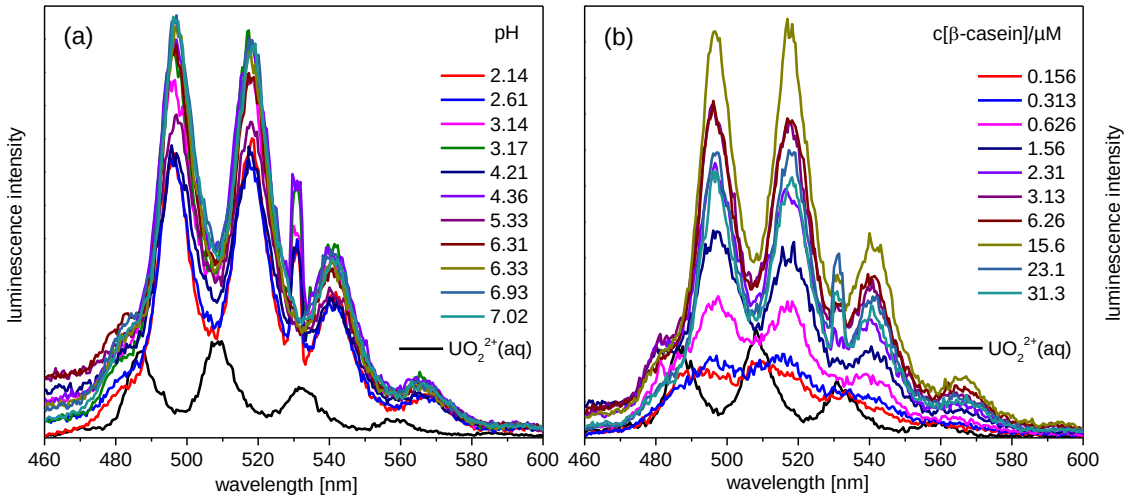

Figure 7. Luminescence spectra of uranium(VI) and β-casein at a uranyl concentration of $1.0 \cdot 10^{-5}$ M (T = 25 °C, I = 0.1 M $NaClO_4$) at 3.13-fold ligand excess in dependence on pH (a) and at pH 4.6 in dependence on ligand concentration (b).

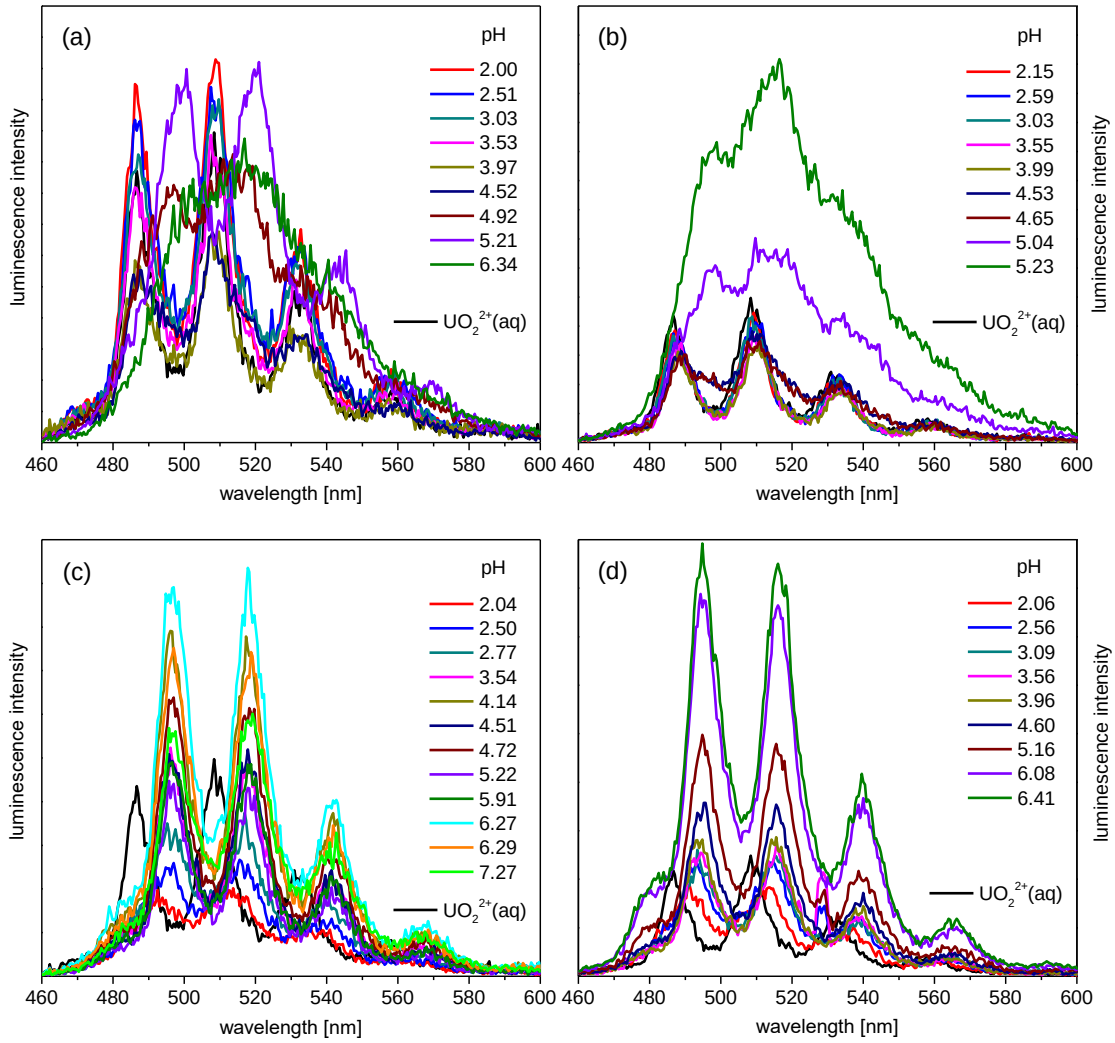

Figure 8. Luminescence spectra of uranium(VI) in dependence of pH at a uranyl concentration of $1.0 \cdot 10^{-5}$ M (T = 25 °C, I = 0.1 M $NaClO_4$) and VESL at 15.6-fold ligand excess (a), VASL at 15.6-fold ligand excess (b), VES^{P}L at 12.0-fold ligand excess (c) and VAS^{P}L at 15.6-fold ligand excess (d).

The luminescence spectra of the peptides without phosphoryl groups, i.e., those of VESL and VASL, show nearly no peak shift at constant peptide concentration and varying pH until a pH value of approximately 4.5. In the case of VASL, raising the pH results in a slight broadening of the peaks; above pH 4.5 an increase in luminescence intensity is observed (Figure 8 a, b). The shapes of the spectra indicate an influence of uranyl hydroxo species and resemble that of uranyl in water at a similar pH,[85] suggesting that nearly no complexation of uranyl with the peptide occurs. VESL shows no increase in luminescence intensity above pH 4.5, and the shapes of the spectra are slightly different from those of VASL (and, consequently, from those of pure UO_2^{2+}), indicating a moderate complexation of uranyl with the carboxylic groups. The different behavior of VASL and VESL is due to the fact that VESL provides twice the number of carboxyl groups than VASL (due to the β-carboxyl group of Glu).

In contrast, VES^{P}L and VAS^{P}L (Figure 8 c, d) cause a significant increase of the luminescence intensity and a red shift of the peak maxima of about 10 nm, compared to pure UO_2^{2+}. This clearly demonstrates that the complex formation of uranyl with the phosphorylated tetrapeptides is much stronger than uranyl complexation with the tetrapeptides having no phosphoryl groups.

The development of the luminescence spectra of the uranyl β-casein system at relatively high β-casein concentration (see Figure 7) is very similar to that of uranyl with VES^{P}L and VAS^{P}L, the phosphorylated tetrapeptides. However, the uranyl β-casein spectra at pH 4.5 and low protein concentration (up to a phosphoryl/uranyl ratio of ~1 : 1) are more comparable to those of uranyl with VESL at pH >4.5. This supports our assumption that the uranyl binding mainly occurs via carboxylic groups at a deficit of phosphoryl groups and at an excess of carboxyl groups, but that the affinity to phosphoryl groups is stronger at higher phosphoryl ratios than that to carboxyl no matter how high the carboxyl ratio is. A similar binding behavior could be shown recently for the interaction of uranium(VI) with the bacterial biomacromolecule lipopolysaccharide.[86]

The luminescence lifetimes were determined from time-resolved spectra. For uranyl plus VASL mono-exponential luminescence decay was observed until pH 4 with a luminescence lifetime of 1.2-1.4 µs which can be assigned to the aqueous UO_2^{2+} species. At pH ≥ 4.5 the decay became bi-exponential with luminescence lifetimes in the range between 4 and 12 µs. They can be assigned to uranyl hydroxo species ($UO_2(OH)_2$: 3.2 µs, $(UO_2)_2(OH)_2^{2+}$: 9.5 µs, $(UO_2)_3(OH)_5^{+}$: 6.6 µs).[85] For VESL again either mono- or bi-exponential luminescence decay was observed. At pH up to ~4 a lifetime of about 1.4 µs can again be assigned to the aqueous UO_2^{2+} species. A second very long lifetime between pH 3 and 4 (25-40 µs) might be caused by the first uranyl hydroxo species UO_2OH^{+} (literature value: 32.8 µs[85]). At pH >4 the first lifetime is slightly shortened up to ~0.6 µs, the second one varies between 7 and 42 µs. This different development of lifetimes for VASL and VESL supports our assumption derived from the luminescence spectra that a moderate complex formation between uranyl and the tetrapeptide only occurs for VESL, but not for VASL.

The uranyl complexes of VES^PL and VAS^PL show mono-exponential luminescence decay, representing probably only one dominating species. The luminescence lifetime of this dominating species is 0.6-1.0 µs, i.e., it is shorter than that of UO_2^{2+} (1.4 µs).

The luminescence decay of uranyl plus casein was always bi-exponential, resulting in a shorter lifetime of 0.6-0.9 µs and a longer one ranging from 4 to 24 µs. However, an assignment of the lifetimes to distinct species is not possible. Equilibria between several uranyl species are to be expected in a uranium(VI) solution containing the highly complex protein which means that the lifetimes derived should be considered as average values. Based on a comparison with the results of the experiments with uranyl plus tetrapeptides, the shorter lifetime might be assigned to phosphoryl complexation, whereas the longer one might belong either to uranyl complexed with carboxyl groups or to further phosphoryl or mixed species. The formation of pure uranyl hydroxo species (without protein coordination) can be ruled out because of the shape of the spectra which clearly points to a dominance of phosphoryl

coordination. These results support and supplement the conclusions drawn from the luminescence spectra.

The TRLFS results show that, beside the dominating phosphoryl coordination, also carboxylate coordination occurs, even though to a minor extent. This is in accordance with the results of the potentiometric titration experiments.

Figure 9 once more demonstrates that, like the adsorption experiments, also our TRLFS experiments reveal the crucial role of the ligands' phosphoryl groups for uranyl binding. In this figure spectra of uranium(VI) in diluted milk and with β-casein, VESL or VES^PL taken at pH 4.6 are combined and compared with the spectrum of UO_2^{2+} (strongly acidic solution). The luminescence intensity was normalized in Figure 9 to facilitate a direct comparison of the spectra with each other. One can see that the uranyl complexes formed in diluted milk, β-casein solution and VES^PL solution (orange-red curves) cause a red shift of the peaks of about 10 nm compared to the pure UO_2^{2+} which is typical for uranyl phosphoryl complexes.[87, 88] The spectrum of the uranyl complex with the phosphoryl-free tetrapeptide VESL (blue curve), on the other hand, shows the same peak positions as that of UO_2^{2+} (black curve) and does not exhibit any peak shift at pH 4.6. This illustrates impressively that the binding of uranium(VI) in milk occurs mainly via the phosphoryl groups of the caseins.

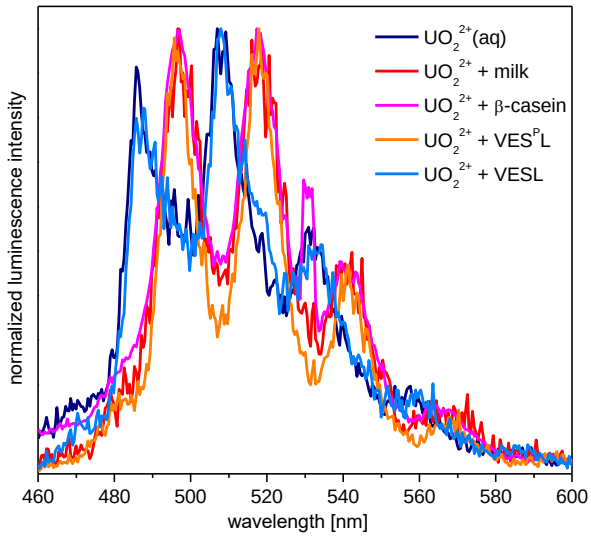

Figure 9. Luminescence spectra of pure UO_2^{2+}, and of uranyl in diluted milk, β-casein, VESL and VES^PL solutions at pH 4.6 and a uranyl concentration of $1.0 \cdot 10^{-5}$ M (T = 25 °C, I = 0.1 M $NaClO_4$). Luminescence intensity is normalized relating to the highest (~510 – 520 nm) peak.

Conclusions

The goal of this study was to contribute to the understanding of uranium(VI) binding to milk proteins, especially the role of the different types of milk proteins and their individual functional groups such as carboxyl and phosphoryl moieties. The combination of different complementary experimental approaches and the unique access to very low uranium(VI) concentrations by means of TRLFS provided an internally consistent description of the system. Considering the different chemical components of milk and their specific interactions with uranium(VI) using a broad range of physico-chemical methods allows conclusions regarding uranyl binding by milk over a relatively wide pH and uranium(VI) concentration range with implications in terms of environment, food, and medicine.

The experiments show a pronounced interaction of uranium(VI) with the studied milk proteins. The equilibrium data of the adsorption process agree well with the Langmuir model. From the Langmuir parameters obtained it can be concluded that the carboxylate groups determine the adsorption capacity, Q_{max}, while the adsorption affinity (as represented by K_L) is mainly controlled by the phosphoserine residues present (or absent) in the proteins. Thus,

the adsorption capacity of the whey proteins is two- to threefold higher than that of the caseins. On the other hand, the Langmuir constants K_L of casein are fivefold higher in H_2O and even 100-fold higher in SMUF than those of the whey proteins. Moreover, in the case of whey protein, the Langmuir parameters Q_{max} and K_L are smaller in SMUF than in H_2O whereas for casein these parameters are comparable for both solutions (c.f. Table 2). SMUF contains free phosphate ions which compete for the formation of stable uranyl complexes with the whey protein molecules that do not possess phosphoryl groups. For the caseins the situation is different since casein itself carries phosphoryl groups. The results for casein suggest a stronger binding of uranyl by protein bound phosphoryl groups in comparison with the free phosphate ions of SMUF, i.e., dissolved phosphate hinders the adsorption of uranium(VI) onto milk proteins without phosphoryl groups but not onto phosphoryl-containing milk proteins. For the latter, even high carbonate concentrations (also in the presence of calcium) have only limited influence on the adsorption process as shown by the experiment with casein and the uranium-rich natural spring water.

The stability of uranyl complexes with phosphoryl-containing, phosphoryl-free and artificially dephosphorylated milk proteins and selected synthetic peptides could be quantified by respective thermodynamic parameters determined by potentiometric titration. The importance of phosphoryl groups for uranium(VI) binding is clearly indicated by the results of the potentiometric titration and supported by TRLFS experiments. It is reflected in the uranium(VI) complex stability constants (Tables 5 to 7) and the resulting uranyl speciation (Figures 5 and 6). In the presence of phosphoryl-containing proteins (i.e., the caseins) there are, even at very low pH, virtually no free UO_2^{2+} ions in solution and no ternary uranyl-hydroxo-protein species are detectable (Figures 5 b, 6 a, b). In contrast, free UO_2^{2+} ions in the acidic region and ternary uranyl hydroxo species in the weakly alkaline region are observed (Figure 6 c) in the case of both dephosphorylated casein and non-phosphorylated peptides.

Finally, the TRLFS experiments illustrate very clearly that it is the phosphoryl group of the milk proteins which preferentially binds the uranyl ion (c.f. Figure 9).

Our findings may open up interesting perspectives for potential practical applications. Both caseins and whey proteins could, for example, be efficient materials for use in water purification. Because of their high affinity for uranium(VI), higher degrees of purification could be achievable with caseins or casein-based adsorbents than with whey proteins. On the other hand, higher sorption capacities and easier regeneration of the loaded sorbent might be possible with whey proteins. Thus, highly efficient single-use sorbents based on caseins and multiple-use sorbents based on whey proteins are conceivable. Furthermore, caseins with their high affinity for uranium(VI) would also be interesting for potential medical purposes, i.e., for the development of uranium(VI) decorporation procedures having only small medical side effects.

Materials and Methods

Materials

All reagents and solvents were obtained commercially and used without further purification except as noted otherwise. Deionized water was boiled to remove carbon dioxide and stored under argon or nitrogen if necessary.

Preparation of proteins and peptides

Separation of "acid casein" and "whey protein". The proteins were obtained from untreated (non-commercial) fresh cow milk since commercial milk which had been treated by heating may have altered its properties (precipitation of calcium phosphate, denaturation of the whey proteins, interaction of the denaturated whey proteins with caseins, dephosphorylation[89, 90]). So-called "acid casein" was obtained by the separation of the casein from the skim milk with the help of precipitation at pH 4.5 as described by Siegl.[91] To this end, the milk was creamed

by centrifuging at 2,200 *g* and 4 °C for 10 minutes. After removing the cream, the obtained skim milk was acidified with a 1 M acetate buffer to adjust a pH of 4.5 which precipitates the casein. The suspension was filtered to remove the liquid (the whey). The separated casein was resuspended in water and the pH of the suspension was adjusted to 7 (NaOH) to redissolve the casein. Then the solution was centrifuged again as described above to remove residual traces of cream. In a similar way, the casein was precipitated, filtered and separated by centrifugation once again. Then the obtained "acid casein" was rinsed with acetone, deep-frozen and freeze-dried. The dried casein was stored at -20 °C. The separated whey, on the other hand, was concentrated using tangential flow filtration and the whey protein after freeze-drying also stored at -20 °C.

Separation of individual casein (ß-casein). Casein in the form of "acid casein" was obtained from fresh milk as described above. The separation of the individual caseins from this casein mixture was accomplished by ion exchange chromatography, as reported by Schwarzenbolz[92] and Menéndez.[93] The purity of the β-casein obtained was >90% as verified by HPLC, determination of nitrogen according to Kjeldahl and gel electrophoresis (SDS-PAGE).[71] The molecular weights of selected caseins and the amino acid composition of β-casein are listed in Tables S1 and S2 (Supporting Information).

Dephosphorylation of casein. A portion of the "acid casein" separated from the milk was dephosphorylated with $Ba(OH)_2$ in alkaline medium using the method developed by Sundararajan.[94] We could remove a fraction of 77% of the phosphoryl groups from the casein within 24 h. The phosphorous concentrations were analyzed by inductively coupled plasma mass spectrometry (ICP-MS, ELAN 9000, Perkin-Elmer, USA).[71]

Synthesis of tetrapeptides. The unphosphorylated peptides VESL, VASL, GESL and VEAL were synthesized by Fmoc solid-phase peptide synthesis (SPPS) techniques from preloaded Fmoc-L-leucine Wang resin (1.1 mmol g^{-1}) in a reaction vessel fitted with a sinter frit.[71, 95] After each coupling step the Fmoc-protecting group was removed and the deprotection

solution was collected and used to estimate the loading by UV/Vis spectrometry at 301 nm (ε = 7,800 M^{-1} L^{-1}). The phosphorylation of VESL, VASL and GESL, resulting in $VES^{P}L$, $VAS^{P}L$ and $GES^{P}L$, was carried out with dibenzyl N,N-diisopropylphosphoramidite and the activator 4,5-dicyanoimidazole. Both reagents were prepared according to literature procedures.[96, 97] For the phosphorylation, the resin was dried *in vacuo* overnight. A mixture of 1.21 g (35 mmol) dibenzyl N,N-diisopropylphosphoramidite and 1.00 g (8.25 mmol) 4,5-dicyanoimidazole in 15 ml dry DMF was added to the dried resin. The reaction vessel was shaken for 8 h under argon, then the solution was drained, the resin washed three times with DMF (10 ml each) and four times with CH_2Cl_2 (10 ml each) and dried again *in vacuo*. The dry resin was covered with 15 ml dry DMF and 3 ml tBuOOH (5.5 M in decane, 16.5 mmol) were added. The reaction vessel was shaken again under argon overnight, then drained and washed again with DMF and CH_2Cl_2 as described above and dried *in vacuo* again.[98]

Cleavage of the unphosphorylated and phosphorylated peptides from resin was performed by stirring with a mixture of trifluoroacetic acid (TFA) : triisopropylsilane (TIS) : water 95 : 2.5 : 2.5 (v : v : v) for several hours. The mixture containing the liberated peptide was concentrated *in vacuo* and the crude product was triturated with cold ether giving the proteins as white or beige solids.[98] The purity of the peptides, monitored with analytical HPLC (high performance liquid chromatography), was between 92 and 100% for the unphosphorylated and between 87 and 97% for the phosphorylated peptides (see Table S8, Supporting Information). The peptides were characterized by ^{1}H- and ^{13}C-NMR and ESI-MS (see Table S8, Supporting Information).

Adsorption experiments

In a *screening experiment* skim milk was produced by centrifugation of commercial (pasteurized and homogenized) milk for 0.5 h at 5,000 *g* and removing the fat fraction. Aliquots of the skim milk were adjusted at room temperature to a) pH 6.7 (the original pH of

milk) and to b) pH 4.6 (the isoelectric point of casein where casein precipitates). Uranium(VI) concentrations of 10^{-7}, 10^{-6}, and 10^{-5} M were adjusted in samples of skim milk aliquots by dissolving $UO_2(NO_3)_2 \cdot 6H_2O$. According to thermodynamic calculations[79] and to experimental data in the literature[99] the solubility limit of uranium(VI) is not exceeded for these concentrations at pH 4.6 (for pH 6.7 it is at least not exceeded for uranium(VI) concentrations of 10^{-7} M and 10^{-6} M). After a reaction time of 20 h (kinetic experiments had shown that the reaction of whey protein with uranium(VI) was finished within a time period of <8 h and that the reaction of casein with uranium(VI) took only about 2 h),[71] the skim milk was divided into 3 fractions by ultracentrifugation for 1 h at 285,000 *g* and ultrafiltration of an aliquot of the supernatant through a 10-kD filter. The fractions are:

a) The centrifugation pellet (mostly casein),

b) The centrifugation supernatant (whey), and

c) The 10-kD ultra filtrate (non-protein constituents such as electrolytes and lactose).

The uranium concentrations in these fractions were analyzed by ICP-MS.

After this screening experiment the *adsorption isotherm of uranium(VI) onto the unseparated milk protein fraction* at pH 4.6 was determined by adjusting uranium(VI) concentrations, c_0, between $5.0 \cdot 10^{-8}$ M and $5.0 \cdot 10^{-5}$ M in diluted skim milk samples. These experiments were done on commercial (pasteurized and homogenized) milk again. The samples were allowed to equilibrate for 3 d. The differentiation between uranium(VI) adsorbed to the milk proteins and free uranium(VI) was performed by 10-kD ultrafiltration and ICP-MS analysis for uranium in the ultra-filtrate. The uranium concentration in the ultra-filtrate is regarded as the equilibrium concentration of free uranium, c_{eq}, at a given point of the adsorption isotherm. The uranium(VI) adsorbed to the milk proteins at this point, Q, is calculated from the uranium concentrations measured before and after ultrafiltration and the adjusted protein concentrations according to:

$$Q = (c_0 - c_{eq})\, V/W \qquad (6)$$

where c_0 (mol L^{-1}) is the uranium(VI) concentration adjusted, V (L) is the volume of the solution and W (g) represents the weight of the milk proteins.

In a next step the *adsorption isotherms of casein and whey protein* separated from untreated (non-commercial) fresh milk were determined separately. To test the influence of the solution environment on the adsorption of uranium(VI) by milk proteins, the experiments were done in both water and simulated milk ultra-filtrate (SMUF) solution. SMUF is used in dairy technology to simulate the electrolyte background of milk. A solution of SMUF was prepared as described[100] with the pH adjusted to 4.6. The composition is listed in Table S3 (Supporting Information). Uranium(VI) solutions were made from $UO_2(NO_3)_2 \cdot 6H_2O$ with concentrations between $1.0 \cdot 10^{-7}$ M and $1.0 \cdot 10^{-5}$ M and at a pH value of 4.6. "Acid casein" or lyophilized whey proteins were suspended in water or in SMUF solution and added to the uranium(VI) solutions leading to concentrations of 14.2 mg L^{-1} casein or 3.2 mg L^{-1} whey protein. The differentiation between uranium(VI) adsorbed to the milk proteins and free uranium(VI) was performed by phase separation using 10-kD ultrafilters and ICP-MS analysis for uranium in the ultra-filtrate and the fraction of adsorbed uranium(VI) was calculated from the uranium(VI) concentration in the ultra-filtrate according to equation (6) again.

In a final experiment the *adsorption power of casein for uranium from uranium-rich natural spring water* (Heinrichsquelle Nürtingen near Stuttgart, Germany)[7] was tested. This water (the spring has been closed meanwhile) contains 371 µg L^{-1} uranium and possesses mineral contents which are unfavorable for uranium adsorption onto casein (carbonate concentration 3.02 g L^{-1}, Ca concentration 53.35 mg L^{-1}, pH 8.3). Tables S4 and S5 (Supporting Information) give our own analyses of the natural spring water. An amount of 1.35 g casein, which corresponds to the casein content of 50 mL milk, was added to a water sample of 50 mL and allowed to react with the uranium at the original pH of the water of 8.3 and after acidification to pH 4.6. The fraction of uranium bound to the casein after reaction was determined by 10-kDa-ultrafiltration and ICP-MS.

Potentiometric titrations

The deprotonation constants of the peptides and proteins as well as the stability constants of the uranyl peptide and uranyl protein complexes were determined at 25 °C in a glove box in N_2 atmosphere (prevention of pH shifts by carbonic acid, prevention of uranyl carbonato complex formation) in a similar way as described in former studies.[101] Ligand titrations in the absence of uranium(VI) were carried out in the pH range between 2 and 12. The ligand concentration was $3.0\ 10^{-3}$ M for the peptides and $3.0\ 10^{-4}$ M for the proteins (the molecular weight was taken as 24 kDa for β-casein, 22.4 kDa for "acid casein", or 21.9 kDa for dephosphorylated "acid casein"; see Table S1, Supporting Information) because the number of functional groups per mass unit is higher in the latter case. Complex stability constants were determined by complexation titrations, i.e., by potentiometric titrations of the organic compounds in the presence of 1.0 mM $UO_2(NO_3)_2$ between pH 2 and 8 to prevent precipitation of uranyl hydroxide species at higher pH values. All titrations were done at least twice up to fivefold with 4.5 mL sample volume each at an ionic strength of 0.1 M ($NaClO_4$) and a HNO_3 concentration of 0.015 M in the initial solutions. Monotonic equivalence point titration was performed automatically in a thermostatic vessel (25.0 ± 0.1 °C) with a 736 GP Titrino device from Metrohm (Herisau, Switzerland) using 0.2 M KOH (carbonate free). The titrating solution was added in constant increments of 0.010 mL each and pH values were measured using a BlueLine glass electrode (Schott) with a minimum drift of 2 mV min^{-1} and a delay time of 120 s after every titration step.

The calculation of the proton binding constants and the complex stability constants from the titration curves was carried out based on Eqn. (2) and (3) or (4) and (5), respectively, with the HYPERQUAD 2003 software.[76] The uranyl hydrolysis constants taken from the respective NEA TDB volume (Table S7, Supporting Information)[18] were included as fixed values. The speciation diagrams were generated either with the code EQ3/6[79] or HySS2006.[80]

Time-resolved laser-induced fluorescence spectroscopy (TRLFS)

The samples were prepared at room temperature in a glove box under inert gas conditions (nitrogen). Two series of measurements were carried out. In the first one the ligand concentration was kept constant ($3.13 \cdot 10^{-5}$ M for β-casein (24 kDa), $1.56 \cdot 10^{-4}$ M for the tetrapeptides VESL, VASL, VES^{P}L and VAS^{P}L) whereas the pH varied between 2 and 7. A constant pH of 4.6 was adjusted in the second series of measurement for β-casein, whereas the protein concentration was varied between $1.56 \cdot 10^{-7}$ and $3.13 \cdot 10^{-5}$ M. In all cases the uranium(VI) concentration was $1.0 \cdot 10^{-5}$ M and the ionic strength was 0.1 M ($NaClO_4$). The luminescence spectra were taken in both the static and the time-resolved modes (excitation wavelength: 266 nm) using a pulsed Nd:YAG laser system (Continuum Minilite Electro-Optics, Inc. Santa Clara, USA) with a delay generator (Delay Generator 8650, EG&G Princeton Instruments New Jersey, USA) and detected using a iHR 550 spectrometer (Horiba Jobin Yvon, Germany), controlled by the accompanying software LabSpec5 (Horiba Jobin Yvon, Germany). In the time-resolved mode the delay times were 200 ns (100 ns in the case of VASL and VAS^{P}L) and 4000 ns, respectively. Spectra within the wavelength range of 371 to 675 nm were recorded. To improve the signal-to-noise ratio, 100 or 200 spectra were accumulated for each sample and an average spectrum calculated.

Acknowledgement

We thank U. Schaefer and C. Eckardt for carrying out the quantitative element- and ion analyses.

Conflicts of interest

The authors declare no competing financial interest.

Supporting Information

Compositions of milk, caseins, and SMUF; analyses of the uranium-rich natural spring water; deprotonation constants of selected amino acids; uranyl hydrolysis constants; characterization of the synthesized tetrapeptides; Langmuir isotherm for whey protein; potentiometric titration curves and speciation diagrams of peptides and proteins with and without uranium(VI).

References

(1) Mkandawire, M. Biogeochemical behaviour and bioremediation of uranium in waters of abandoned mines. *Environ. Sci. Pollut. Res.* **2013,** *20*, 7740-7767.

(2) Waseem, A.; Ullah, H.; Rauf, M. K.; Ahmad, I. Distribution of Natural Uranium in Surface and Groundwater Resources: A Review. *Crit. Rev. Environ. Sci. Technol.* **2015,** *45*, 2391-2423.

(3) Bjorklund, G.; Christophersen, O. A.; Chirumbolo, S.; Selinus, E.; Aaseth, J. Recent aspects of uranium toxicology in medical geology. *Environ. Res.* **2017,** *156*, 526-533.

(4) WHO, *Guidelines for Drinking-water Quality*. World Health Organization, 2011; p 564.

(5) WHO, *Uranium in Drinking-water. Background document for development of WHO Guidelines for Drinking-water Quality*. World Health Organization, 2011; p 29.

(6) Ansoborlo, E.; Lebaron-Jacobs, L.; Prat, O. Uranium in drinking-water: A unique case of guideline value increases and discrepancies between chemical and radiochemical guidelines. *Environ. Int.* **2015,** *77*, 1-4.

(7) Knolle, F.; Schnug, E.; Birke, M.; Hassoun, R.; Jacobs, F., Uranium in German Mineral Water – Occurrence and Origins. In *The New Uranium Mining Boom*, Merkel, B.; Schipek, M., Eds. Springer Geology: 2012; pp 749-754.

(8) Schnug, E.; Lottermoser, B. G. Fertilizer-Derived Uranium and its Threat to Human Health. *Environ. Sci. Technol.* **2013,** *47*, 2433-2434.

(9) Avelar, A. C.; Ferreira, W. M.; Pemberthy, D.; Abad, E.; Amaral, M. A. Dioxins, furans, biphenyls, arsenic, thorium and uranium in natural and anthropogenic sources of phosphorus and calcium used in agriculture. *Sci. Total Environ.* **2016,** *551*, 695-698.

(10) Katz, S. A. The Chemistry and Toxicology of Depleted Uranium. *Toxics* **2014,** *2*, 50-78.

(11) Faa, A.; Gerosa, C.; Fanni, D.; Floris, G.; Eyken, P. V.; Lachowicz, J. I.; Nurchi, V. M. Depleted Uranium and Human Health. *Curr. Med. Chem.* **2018,** *25*, 49-64.

(12) Burns, P. C.; Ewing, R. C.; Navrotsky, A. Nuclear Fuel in a Reactor Accident. *Science* **2012,** *335*, 1184-1188.

(13) Shinonaga, T.; Steier, P.; Lagos, M.; Ohkura, T. Airborne Plutonium and Non-Natural Uranium from the Fukushima DNPP Found at 120 km Distance a Few Days after Reactor Hydrogen Explosions. *Environ. Sci. Technol.* **2014,** *48*, 3808-3814.

(14) Lucena, A. F.; Carretas, J. M.; Marcalo, J.; Michelini, M. D.; Rutkowski, P. X.; Gibson, J. K. Dissociation of Gas-Phase Bimetallic Clusters as a Probe of Charge Densities: The Effective Charge of Uranyl. *J. Phys. Chem. A* **2014,** *118*, 2159-2166.

(15) Pearson, R. G. Hard and Soft Acids and Bases HSAB, Part 1, Fundamental Principles. *J. Chem. Educ.* **1968,** *45*, 581-587.

(16) Altmaier, M.; Gaona, X.; Fanghänel, T. Recent advances in aqueous actinide chemistry and thermodynamics. *Chem. Rev.* **2013,** *113*, 901-43.

(17) Maher, K.; Bargar, J. R.; Brown, G. E. Environmental Speciation of Actinides. *Inorg. Chem.* **2013,** *52*, 3510-3532.

(18) Guillaumont, R.; Fanghänel, T.; Fuger, J.; Grenthe, I.; Neck, V.; Palmer, D. A.; Rand, M. H., *Update on the Chemical Thermodynamics of Uranium, Neptunium, Plutonium, Americium and Technetium.* Elsevier: Amsterdam, 2003.

(19) Berto, S.; Crea, F.; Daniele, P. G.; Gianguzza, A.; Pettignano, A.; Sammartano, S. Advances in the investigation of dioxouranium(VI) complexes of interest for natural fluids. *Coord. Chem. Rev.* **2012,** *256*, 63-81.

(20) Gorden, A. E.; Xu, J.; Raymond, K. N.; Durbin, P. Rational design of sequestering agents for plutonium and other actinides. *Chem. Rev.* **2003,** *103*, 4207-4282.

(21) Van Horn, J. D.; Huang, H. Uranium(VI) bio-coordination chemistry from biochemical, solution and protein structural data. *Coord. Chem. Rev.* **2006**, 765-775.

(22) Vidaud, C.; Gourion-Arsiquaud, S.; Rollin-Genetet, F.; Torne-Celer, C.; Plantevin, S.; Pible, O.; Berthomieu, C.; Quemeneur, E. Structural consequences of binding of UO_2^{2+} to apotransferrin: Can this protein account for entry of uranium into human cells? *Biochemistry* **2007,** *46*, 2215-2226.

(23) Basset, C.; Averseng, O.; Ferron, P. J.; Richaud, N.; Hagege, A.; Pible, O.; Vidaud, C. Revision of the Biodistribution of Uranyl in Serum: Is Fetuin-A the Major Protein Target? *Chem. Res. Toxicol.* **2013,** *26*, 645-653.

(24) Ali, M.; Kumar, A.; Kumar, M.; Pandey, B. N. The interaction of human serum albumin with selected lanthanide and actinide ions: Binding affinities, protein unfolding and conformational changes. *Biochimie* **2016,** *123*, 117-129.

(25) Kumar, A.; Ali, M.; Ningthoujam, R. S.; Gaikwad, P.; Kumar, M.; Nath, B. B.; Pandey, B. N. The interaction of actinide and lanthanide ions with hemoglobin and its relevance to human and environmental toxicology. *J. Hazard. Mater.* **2016,** *307*, 281-293.

(26) Odoh, S. O.; Bondarevsky, G. D.; Karpus, J.; Cui, Q.; He, C.; Spezia, R.; Gagliardi, L. UO_2^{2+} Uptake by Proteins: Understanding the Binding Features of the Super Uranyl Binding Protein and Design of a Protein with Higher Affinity. *J. Am. Chem. Soc.* **2014,** *136*, 17484-17494.

(27) Safi, S.; Jeanson, A.; Roques, J.; Solari, P. L.; Charnay-Pouget, F.; Den Auwer, C.; Creff, G.; Aitken, D. J.; Simoni, E. Thermodynamic and Structural Investigation of Synthetic Actinide-Peptide Scaffolds. *Inorg. Chem.* **2016,** *55*, 877-886.

(28) Barkleit, A.; Hennig, C.; Ikeda-Ohno, A. Interaction of Uranium(VI) with α-Amylase and Its Implication for Enzyme Activity. *Chem. Res. Toxicol.* **2018,** *31*, 1032-1041.

(29) Li, B.; Raff, J.; Barkleit, A.; Bernhard, G.; Foerstendorf, H. Complexation of U(VI) with highly phosphorylated protein, phosvitin: A vibrational spectroscopic approach. *J. Inorg. Biochem.* **2010,** *104*, 718-725.

(30) Pardoux, R.; Sauge-Merle, S.; Lemaire, D.; Delangle, P.; Guilloreau, L.; Adriano, J. M.; Berthomieu, C. Modulating Uranium Binding Affinity in Engineered Calmodulin EF-Hand Peptides: Effect of Phosphorylation. *PLoS One* **2012,** *7*.

(31) Qi, L.; Basset, C.; Averseng, O.; Quemeneur, E.; Hagege, A.; Vidaud, C. Characterization of UO_2^{2+} binding to osteopontin, a highly phosphorylated protein: insights into potential mechanisms of uranyl accumulation in bones. *Metallomics* **2014,** *6*, 166-176.

(32) Sauge-Merle, S.; Brulfert, F.; Pardoux, R.; Solari, P. L.; Lemaire, D.; Safi, S.; Guilbaud, P.; Simoni, E.; Merroun, M. L.; Berthomieu, C. Structural Analysis of Uranyl Complexation by the EF-Hand Motif of Calmodulin: Effect of Phosphorylation. *Chem. Eur. J.* **2017,** *23*, 15505-15517.

(33) Starck, M.; Sisommay, N.; Laporte, F. A.; Oros, S.; Lebrun, C.; Delangle, P. Preorganized Peptide Scaffolds as Mimics of Phosphorylated Proteins Binding Sites with a High Affinity for Uranyl. *Inorg. Chem.* **2015,** *54*, 11557-11562.

(34) Lebrun, C.; Starck, M.; Gathu, V.; Chenavier, Y.; Delangle, P. Engineering Short Peptide Sequences for Uranyl Binding. *Chem. Eur. J.* **2014,** *20*, 16566-16573.

(35) Starck, M.; Laporte, F. A.; Oros, S.; Sisommay, N.; Gathu, V.; Solari, P. L.; Creff, G.; Roques, J.; Den Auwer, C.; Lebrun, C.; Delangle, P. Cyclic Phosphopeptides to Rationalize

the Role of Phosphoamino Acids in Uranyl Binding to Biological Targets. *Chem. Eur. J.* **2017,** *23*, 5281-5290.

(36) Anke, M.; Seeber, O.; Müller, R.; Schäfer, U.; Zerull, J. Uranium transfer in the food chain from soil to plants, animals and man. *Chem. Erde* **2009,** *69*, 75-90.

(37) Pearson, A. J.; Gaw, S.; Hermanspahn, N.; Glover, C. N. Natural and anthropogenic radionuclide activity concentrations in the New Zealand diet. *J. Environ. Radioact.* **2016,** *151*, 601-608.

(38) Kumar, M.; Prasher, S.; Singh, S. Uranium analysis in some food samples collected from Bathinda area of Punjab, India. *Indian J. Phys.* **2009,** *83*, 1045-1050.

(39) Gigli, I., *Milk Proteins - From Structure to Biological Properties and Health Aspects*. IntechOpen: Rijeka, Croatia, 2016.

(40) Park, Y. W.; Nam, M. S. Bioactive Peptides in Milk and Dairy Products: A Review. *Korean J. Food Sci. Anim. Resour.* **2015,** *35*, 831-840.

(41) Farrell, H. M.; Malin, E. L.; Brown, E. M.; Qi, P. X. Casein micelle structure: What can be learned from milk synthesis and structural biology? *Curr. Opin. Colloid Interface Sci.* **2006,** *11*, 135-147.

(42) Garcia, J. S.; de Magalhaes, C. S.; Arruda, M. A. Z. Trends in metal-binding and metalloprotein analysis. *Talanta* **2006,** *69*, 1-15.

(43) Mishra, S. P.; Tiwari, D.; Dubey, R. S.; Mishra, M. Biosorptive behaviour of casein for Zn^{2+}, Hg^{2+} and Cr^{3+}: Effects of physico-chemical treatments. *Bioresour. Technol.* **1998,** *63*, 1-5.

(44) Pomastowski, P.; Sprynskyy, M.; Buszewski, B. The study of zinc ions binding to casein. *Colloid Surf. B-Biointerfaces* **2014,** *120*, 21-27.

(45) Yamada, M.; Tsuruzumi, M. Utilization of milk protein as an environmental material: accumulation of metal ions using a protein-inorganic hybrid material. *Polym. J.* **2016,** *48*, 295-300.

(46) Bolisetty, S.; Mezzenga, R. Amyloid-carbon hybrid membranes for universal water purification. *Nat. Nanotechnol.* **2016,** *11*, 365-372.

(47) Joksic, A. S.; Katz, S. A. Chelation therapy for treatment of systemic intoxication with uranium: A review. *J. Environ. Sci. Health, Pt. A: Toxic/Hazard. Subst. Environ. Eng.* **2015,** *50*, 1479-88.

(48) Lawrence, G. D.; Patel, K. S.; Nusbaum, A. Uranium toxicity and chelation therapy. *Pure Appl. Chem.* **2014,** *86*, 1105-1110.

(49) Chen, A. W.; Shang, C.; Shao, J. H.; Zhang, J. C.; Huang, H. L. The application of iron-based technologies in uranium remediation: A review. *Sci. Total Environ.* **2017,** *575*, 1291-1306.

(50) Aly, M. M.; Hamza, M. F. A Review: Studies on Uranium Removal Using Different Techniques. Overview. *J. Dispersion Sci. Technol.* **2013,** *34*, 182-213.

(51) Schierz, A.; Zänker, H. Aqueous suspensions of carbon nanotubes: Surface oxidation, colloidal stability and uranium sorption. *Environ. Pollut.* **2009,** *157*, 1088-1094.

(52) Kim, J.; Tsouris, C.; Mayes, R. T.; Oyola, Y.; Saito, T.; Janke, C. J.; Dai, S.; Schneider, E.; Sachde, D. Recovery of Uranium from Seawater: A Review of Current Status and Future Research Needs. *Sep. Sci. Technol.* **2013,** *48*, 367-387.

(53) Kou, S. Z.; Yang, Z. G.; Sun, F. Protein Hydrogel Microbeads for Selective Uranium Mining from Seawater. *ACS Appl. Mater. Interfaces* **2017,** *9*, 2035-2039.

(54) Abney, C. W.; Mayes, R. T.; Saito, T.; Dai, S. Materials for the Recovery of Uranium from Seawater. *Chem. Rev.* **2017,** *117*, 13935-14013.

(55) Parker, B. F.; Zhang, Z.; Rao, L.; Arnold, J. An overview and recent progress in the chemistry of uranium extraction from seawater. *Dalton Trans.* **2018,** *47*, 639-644.

(56) Feng, M. L.; Sarma, D.; Qi, X. H.; Du, K. Z.; Huang, X. Y.; Kanatzidis, M. G. Efficient Removal and Recovery of Uranium by a Layered Organic-Inorganic Hybrid Thiostannate. *J. Am. Chem. Soc.* **2016,** *138*, 12578-12585.

(57) Ling, L.; Zhang, W. X. Enrichment and Encapsulation of Uranium with Iron Nanoparticle. *J. Am. Chem. Soc.* **2015,** *137*, 2788-2791.

(58) Ma, S. L.; Huang, L.; Ma, L. J.; Shim, Y.; Islam, S. M.; Wang, P. L.; Zhao, L. D.; Wang, S. C.; Sun, G. B.; Yang, X. J.; Kanatzidis, M. G. Efficient Uranium Capture by Polysulfide/Layered Double Hydroxide Composites. *J. Am. Chem. Soc*. **2015,** *137*, 3670-3677.

(59) Manos, M. J.; Kanatzidis, M. G. Layered Metal Sulfides Capture Uranium from Seawater. *J. Am. Chem. Soc.* **2012,** *134*, 16441-16446.

(60) Sun, Q.; Aguila, B.; Perman, J.; Ivanov, A. S.; Bryantsev, V. S.; Earl, L. D.; Abney, C. W.; Wojtas, L.; Ma, S. Bio-inspired nano-traps for uranium extraction from seawater and recovery from nuclear waste. *Nat. Commun.* **2018,** *9*, 1644.

(61) Sun, X.; Huang, X.; Liao, X. P.; Shi, B. Adsorptive recovery of UO_2^{2+} from aqueous solutions using collagen-tannin resin. *J. Hazard. Mater.* **2010,** *179*, 295-302.

(62) Muzzarelli, R. A. A. Potential of chitin/chitosan-bearing materials for uranium recovery: An interdisciplinary review. *Carbohydr. Polym.* **2011,** *84*, 54-63.

(63) Das, N. Remediation of Radionuclide Pollutants through Biosorption - an Overview. *Clean-Soil Air Water* **2012,** *40*, 16-23.

(64) Zhou, L.; Bosscher, M.; Zhang, C. S.; Ozcubukcu, S.; Zhang, L.; Zhang, W.; Li, C. J.; Liu, J. Z.; Jensen, M. P.; Lai, L. H.; He, C. A protein engineered to bind uranyl selectively and with femtomolar affinity. *Nat. Chem.* **2014,** *6*, 236-241.

(65) Baum, F.; Fedorova, M.; Ebner, J.; Hoffmann, R.; Pischetsrieder, M. Analysis of the Endogenous Peptide Profile of Milk: Identification of 248 Mainly Casein-Derived Peptides. *J. Proteome Res.* **2013,** *12*, 5447-5462.

(66) Partschefeld, C.; Schwarzenbolz, U.; Richter, S.; Henle, T. Crosslinking of casein by microbial transglutaminase and its resulting influence on the stability of micelle structure. *Biotechnol. J.* **2007,** *2*, 456-461.

(67) Schlimme, E.; Buchheim, W., *Milch und ihre Inhaltsstoffe – Chemische und physikalische Eigenschaften*. 2 ed.; Verlag Th. Mann: Gelsenkirchen (in German), 1999.

(68) Stumm, W., *Chemistry of the Solid-Water Interface: Processes at the Mineral-Water and Particle-Water Interface in Natural Systems*. Wiley-Interscience: New York, 1992.

(69) Qi, P. X.; Brown, E. M.; Farrell, H. M. 'New views' on structure-function relationships in milk proteins. *Trends Food Sci. Technol.* **2001,** *12*, 339-346.

(70) Prat, O.; Vercouter, T.; Ansoborlo, E.; Fichet, P.; Perret, P.; Kurttio, P.; Salonen, L. Uranium Speciation in Drinking Water from Drilled Wells in Southern Finland and Its Potential Links to Health Effects. *Environ. Sci. Technol.* **2009,** *43*, 3941-3946.

(71) Heine, K. B. U(VI) binding onto milk proteins and model peptides. PhD thesis,Technische Universität Dresden, Germany (in German), 2016.

(72) Österberg, R. Phosphorus linkages in alpha-casein. *Biochim. Biophys. Acta* **1961,** *54*, 424-431.

(73) Aleksandrov, A.; Polydorides, S.; Archontis, G.; Simonson, T. Predicting the Acid/Base Behavior of Proteins: A Constant-pH Monte Carlo Approach with Generalized Born Solvent. *J. Phys. Chem. B* **2010,** *114*, 10634-10648.

(74) Chruscinski, L.; Dyba, M.; JezowskaBojczuk, M.; Kozlowski, H.; Kupryszewski, G.; Mackiewicz, Z.; Majewska, A. Specific interactions of Cu^{2+} ions with fragments of envelope protein of hepatitis B virus. *J. Inorg. Biochem.* **1996,** *63*, 49-55.

(75) Villa, F.; Simonson, T. Protein pK(a)'s from Adaptive Landscape Flattening Instead of Constant-pH Simulations. *J. Chem. Theory Comput.* **2018,** *14*, 6714-6721.

(76) Gans, P.; Sabatini, A.; Vacca, A. Investigation of equilibria in solution. Determination of equilibrium constants with the HYPERQUAD suite of programs. *Talanta* **1996,** *43*, 1739-1753.

(77) Kallay, C.; Varnagy, K.; Micera, G.; Sanna, D.; Sovago, I. Copper(II) complexes of oligopeptides containing aspartyl and glutamyl residues. Potentiometric and spectroscopic studies. *J. Inorg. Biochem.* **2005,** *99*, 1514-1525.

(78) Kallay, C.; Sovago, I.; Varnagy, K. Nickel(II) complexes of oligopeptides containing aspartyl and glutamyl residues. Potentiometric and spectroscopic studies. *Polyhedron* **2007,** *26*, 811-817.

(79) Wolery, T. J. *EQ3/6. A software package for the geochemical modeling of aqueous systems*, CA (USA): 1992.

(80) Alderighi, L.; Gans, P.; Ienco, A.; Peters, D.; Sabatini, A.; Vacca, A. Hyperquad simulation and speciation (HySS): a utility program for the investigation of equilibria involving soluble and partially soluble species. *Coord. Chem. Rev.* **1999,** *184*, 311-318.

(81) Kannan, S.; Kumar, M.; Sadhu, B.; Jaccob, M.; Sundararajan, M. Unusual intramolecular CH···O hydrogen bonding interaction between a sterically bulky amide and uranyl oxygen. *Dalton Trans.* **2017,** *46*, 16939-16946.

(82) Sovago, I.; Kallay, C.; Varnagy, K. Peptides as complexing agents: Factors influencing the structure and thermodynamic stability of peptide complexes. *Coord. Chem. Rev.* **2012,** *256*, 2225-2233.

(83) Dudev, T.; Lim, C. Competition among Metal Ions for Protein Binding Sites: Determinants of Metal Ion Selectivity in Proteins. *Chem. Rev.* **2014,** *114*, 538-556.

(84) Kozlowski, H.; Potocki, S.; Remelli, M.; Rowinska-Zyrek, M.; Valensin, D. Specific metal ion binding sites in unstructured regions of proteins. *Coord. Chem. Rev.* **2013,** *257*, 2625-2638.

(85) Eliet, V.; Bidoglio, G.; Omenetto, N.; Parma, L.; Grenthe, I. Characterization of Hydroxide Complexes of Uranium(VI) by Time-Resolved Fluorescence Spectroscopy. *J. Chem. Soc., Faraday Trans.* **1995,** *91*, 2275-2285.

(86) Barkleit, A.; Foerstendorf, H.; Li, B.; Rossberg, A.; Moll, H.; Bernhard, G. Coordination of uranium(VI) with functional groups of bacterial lipopolysaccharide studied by EXAFS and FT-IR spectroscopy. *Dalton Trans.* **2011,** *40*, 9868-9876.

(87) Barkleit, A.; Moll, H.; Bernhard, G. Interaction of uranium(VI) with lipopolysaccharide. *Dalton Trans.* **2008**, 2879-2886.

(88) Koban, A.; Bernhard, G. Uranium(VI) complexes with phospholipid model compounds - a laser spectroscopic study. *J. Inorg. Biochem.* **2007,** *101*, 750-7.

(89) Fox, P. F. Heat-induced changes in milk preceding coagulation. *J. Dairy Sci.* **1981,** *64*, 2127-2137.

(90) Aoki, T.; Umeda, T.; Kako, Y. Cleavage of the linkage between colloidal calcium-phosphate and casein on heating milk at high-temperature. *J. Dairy Res.* **1990,** *57*, 349-354.

(91) Siegl, T. Studies to the crosslinking of milk proteins and the formation of individual crosslinking amino acids. PhD thesis, Technische Universität Dresden, Germany (in German), 2003.

(92) Schwarzenbolz, U. Studies to non-enzymatic glycosylation and crosslinking of milk proteins. PhD thesis,Technische Universität München, Germany (in German), 2000.

(93) Menéndez, O. Stability of microbial transglutaminase and its reactions with individual caseins under atmospheric and high pressure. PhD thesis, Technische Universität Dresden, Germany, 2006.

(94) Sundararajan, T. A.; Kumar, K.; Sarma, P. S. Role of cation in the dephosphorylation of phosphoproteins by alkali. *Biochim. Biophys. Acta* **1958,** *28*, 148-158.

(95) Merrifield, R. B. Solid phase peptide synthesis. 1. Synthesis of a tetrapeptide. *J. Am. Chem. Soc.* **1963,** *85*, 2149-2154.

(96) Andrews, D. M.; Kitchin, J.; Seale, P. W. Solid-Phase Synthesis of a Range of O-Phosphorylated Peptides by Post-Assembly Phosphitylation and Oxidation. *Int. J. Pept. Protein Res.* **1991,** *38*, 469-475.

(97) Oconnell, J. F.; Parquette, J.; Yelle, W. E.; Wang, W.; Rapoport, H. Convenient Synthesis of Methyl 1-Methyl-2,4-Dibromo-5-Imidazolecarboxylate. *Synthesis* **1988**, 767-771.

(98) Heine, K. B.; Fairweather, K. A.; Heine, A.; Clegg, J. K.; Jolliffe, K. A.; Gloe, K.; Gloe, K.; Bernhard, G.; Henle, T. Unusual Absence of Head-to-Tail Chains in the Crystal Structure of Glycyl-L-glutamyl-L-phosphoseryl-L-leucine. *J. Chem. Crystallogr.* **2012,** *42*, 839-845.

(99) Jung, E. C.; Cho, H. R.; Park, K. K.; Yeon, J. W.; Song, K. Nanoparticle sizing by a laser-induced breakdown detection using an optical probe beam deflection. *Appl. Phys. B-Lasers Opt.* **2009,** *97*, 867-875.

(100) Jenness, R.; Koops, J. Preparation and properties of a salt solution which simulates milk ultrafiltrate. *Neth. Milk Dairy J.* **1962,** *16*, 153-164.

(101) Heine, K. B.; Clegg, J. K.; Heine, A.; Gloe, K.; Gloe, K.; Henle, T.; Bernhard, G.; Cai, Z. L.; Reimers, J. R.; Lindoy, L. F.; Lach, J.; Kersting, B. Complexation, computational, magnetic, and structural studies of the Maillard reaction product isomaltol including investigation of an uncommon pi interaction with copper(II). *Inorg. Chem.* **2011,** *50*, 1498-505.

For Table of Contents Only

Graphical Abstract

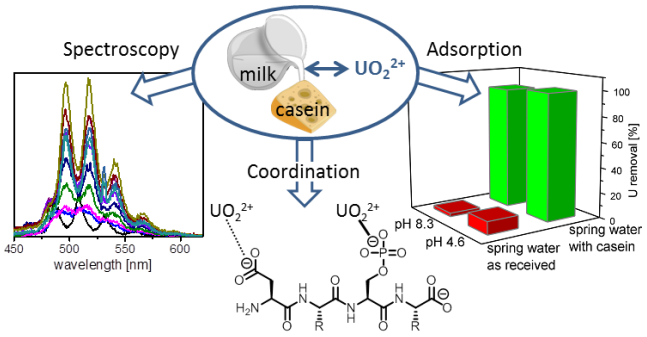

Synopsis

Bovine milk proteins (caseins and whey proteins) are able to catch high amounts of uranium from water. Particularly the phosphoryl groups of the caseins have a very high binding affinity towards uranium, whereas the high amount of carboxyl groups, especially in whey proteins, is responsible for a high sorption capacity. Both caseins and whey could be cheap and efficient materials for water purification.

Supporting Information (SI)

Strong Uranium(VI) Binding onto Bovine Milk Proteins, Selected Protein Sequences and Model peptides

Harald Zänker,[a] Katja Heine,[a,b,#] Stephan Weiss,[a] Vinzenz Brendler,[a] Richard Husar,[a] Gert Bernhard,[a] Karsten Gloe,[b] Thomas Henle,[b] Astrid Barkleit,[a,*]

[a] Helmholtz-Zentrum Dresden - Rossendorf, Institute of Resource Ecology, Bautzner Landstraße 400, 01328 Dresden, Germany

[b] Technische Universität Dresden, Faculty of Chemistry and Food Chemistry, 01062 Dresden, Germany

Present address: Berliner Glas, Waldkraiburger Straße 5, 12347 Berlin, Germany

* Corresponding author. E-Mail: a.barkleit@hzdr.de

Tables

Table S1. Composition of bovine casein and amount of phosphoserine (P-Ser) per molecule.[1-4]

Protein	% of whole casein [4]	MW [kDa]	Number of P-Ser residues [4]
α_{S1}-casein	38	23.6	8
α_{S2}-casein	10	23.2	11
β-casein	40	24	5
κ-casein	12	19	1
"acid casein"[3]		~22.4	~6
dephos. casein[3]		~21.9	~1

Table S2. Amino acid composition of β-casein.[1]

Amino acid residue	Number	Amino acid residue	Number
Ala (A)	5	Lys (K)	11
Arg (R)	4	Met (M)	6
Asn (N)	5	Phe (F)	9
Asp (D)	4	Pro (P)	35
Gln (Q)	20	Ser (S)	11
Glu (E)	19	P-Ser (S^P)	5
Gly (G)	5	Thr (T)	9
His (H)	5	Trp (W)	1
Ile (I)	10	Tyr (Y)	4
Leu (L)	22	Val (V)	19

Table S3. Composition of simulated milk ultrafiltrate (SMUF) solution.[5]

Ingredient	Weight	Composition [mg (100 mL)$^{-1}$]								
	[g L^{-1}]	Na	K	Ca	Mg	P	Cl	citrate	SO_4	CO_3
KH_2PO_4	1.58		45.4			36.0				
K_3citrate·H_2O	1.20		43.4					70.0		
Na_3citrate·$5H_2O$	2.12	42.0						115.1		
K_2SO_4	0.18		8.0						9.9	
$CaCl_2·2H_2O$	1.32			35.9			63.8			
$MgCl_2·6H_2O$	0.65				7.8		22.7			
K_2CO_3	0.30		17.0							9.5
KCl	0.60		31.4				28.5			
KOH to pH 6.6	2.25 m-eq		8.8							
Total	mg (100 mL)$^{-1}$	42.0	154.0	35.9	7.8	36.0	115.0	185.1	9.9	9.5
	mM L^{-1}	18.3	39.4	9.0	3.2	11.6	32.4	9.6	1.0	2.2

Table S4. Content of selected elements in the natural spring water Heinrichsquelle Nürtingen (analyses made by the authors).[3]

Component	Concentration [µg L^{-1}]
B	1,330.0
Na	22,900,000.0
Mg	41,300.0
Al	2.7
Si	7,365.0
P	76.5
K	36,500.0
Ca	53,350.0
Mn	10.9
Co	0.3
Ni	6.2
Cu	25.9
Zn	34.2
Se	≤1
Sr	964.0
Mo	1.9
Cs	0.5
Ba	7.9
U	371.0

Table S5. Content of selected anions and total organic carbon (TOC) in the natural spring water Heinrichsquelle Nürtingen (analyses made by the authors).[3]

Component	Concentration [mg L^{-1}]
F^-	0.5
Cl^-	420.0
NO_2^-	≤ 0.2
NO_3^-	16.1
PO_4^{3-}	≤ 0.5
SO_4^{2-}	3065.0
CO_3^{2-}	3020.0
TOC	1.5

Table S6. Stepwise deprotonation constants of the amino acids L-glutamic acid (Glu), L-serine (Ser) and L-phosphoserine (P-Ser) determined by potentiometric titration at T = 25 °C and I = 0.1 M ($NaClO_4$). Errors of the last significant decimal place (σ) are given in parentheses.[3]

	pK_a				
	$-OPO_3H_2$	α-COOH	γ-COOH	$-OPO_3H^-$	α-NH_3^+
Glu		2.38(1)	4.23(1)		9.49(1)
Ser		2.08(1)	8.72[6]		9.06(1)
P-Ser	1.19(3)	1.94(1)	9.93[7]	5.72(2)	7.86(1)

Table S7. Thermodynamic stability constants for aqueous uranyl complexes that are used for stability constant calculation and speciation modelling.[8]

Uranyl complex	$\log ß_{I=0M,\ T=25°C}$	Uncertainty (±)
UO_2OH^+	-5.250	0.240
$UO_2(OH)_{2(aq)}$	-12.150	0.070
$(UO_2)(OH)_2^{2+}$	-5.620	0.040
$UO_2(OH)_3^-$	-20.250	0.420
$UO_2(OH)_4^{2-}$	-32.400	0.680
$(UO_2)_2OH^{3+}$	-2.700	1.000
$(UO_2)_3(OH)_4^{2+}$	11.900	0.300
$(UO_2)_3(OH)_5^+$	-15.550	0.120
$(UO_2)_3(OH)_7^-$	-32.200	0.800
$(UO_2)_4(OH)_7^+$	-21.900	1.000
$UO_2(CO_3)_2^{2-}$	16.610	0.090
$UO_2(CO_3)_3^{4-}$	21.840	0.040
$(UO_2)_2CO_3(OH)_3^-$	-0.858	0.851
$(UO_2)_3(CO_3)_6^{6-}$	54.000	1.000

Table S8. Characterization of the synthesized tetrapeptides.

Peptide	Purity[a]	^{1}H NMR[b] δ [ppm]	^{13}C NMR[c] δ [ppm]	MS[d] [m/z]
VESL	100.0	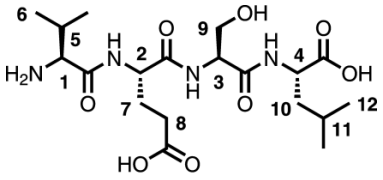 0.94 (dd, J = 15.41, 6.50 Hz, 6H, 12-H), 1.05 (dd, J = 15.18, 6.90 Hz, 6H, 6-H), 1.60-1.68 (m, 2H, 10-H), 1.68-1.79 (m, 1H, 11-H), 1.92-2.03 (m, 1H, 5-H), 2.10-2.26 (m,2H, 7-H), 2.39-2.50 (m, 2H, 8-H), 3.71 (d, J = 5.62 Hz, 1H, 1-H), 3.79 (dd, J = 5.63, 1.27 Hz, 2H, 9-H), 4.42-4.55 (m, 3H, 2-H, 3-H, 4-H)	17.9, 18.9, 21.9, 23.4, 25.9, 28.4, 31.0, 31.6, 52.2, 54.1, 56.7, 59.6, 63.1, 66.9, 169.7, 172.1, 173.0, 175.9, 176.5	893.6 ([2M+H]$^{+}$, 100 %), 447.3 ([M+H]$^{+}$, 25 %
VASL	98.3	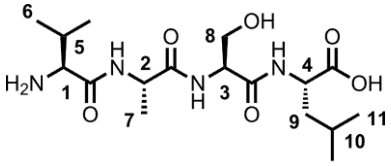 0.94 (dd, J = 15.67, 6.47 Hz, 6H, 11-H), 1.06 (dd, J = 16.13, 6.92 Hz, 6H, 6-H), 1.41 (d, J = 7.14 Hz, 3H, 7-H), 1.61-1.68 (m, 2H, 9-H), 1.68-1.77 (m, 1H, 10-H), 2.21-2.27 (qd, J = 13.73, 6.88 Hz 1H, 5-H), 3.69 (d, J = 5.76 Hz, 1H, 1-H), 3.79 (d, J = 5.48 Hz, 2H, 8-H), 4.42-4.50 (m, 3H, 2-H, 3-H, 4-H)	18.3, 18.9, 19.7, 22.7, 24.2, 26.8, 32.2, 42.5, 51.7, 53.0, 57.6, 60.7, 62.5, 170.7, 173.0, 175.8, 177.0	389 ([M+H]$^{+}$ 100%), 777 ([2M+H]$^{+}$ 63.8%), 799 ([2M+Na]$^{+}$ 9.4%)
GESL	91.9	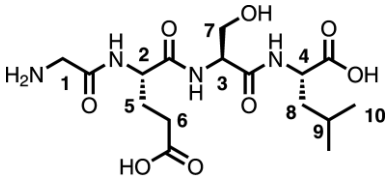 0.95 (dd, J = 12.84, 6.40 Hz, 6H, 10-H), 1.62-1.68 (m, 2H, 8-H), 1.68-1.80 (m, 1H, 9-H), 1.90-2.02 (m, 1H, 5-Ha), 2.09-2.21 (m, 1H, 5-Hb), 2.43 (t, J = 7.6 Hz, 2H, 6-H), 3.73 (s, 2H, 1-H), 3.77-3.81 (m, 2H, 7-H), 4.42-4.55 (m, 3H, 2-H, 3-H, 4-H)	21.9, 23.3, 26.0, 28.5, 31.0, 41.5, 41.7, 52.2, 54.1, 56.6, 63.1, 167.5, 172.1, 173.3, 175.9, 176.4	405 ([M+H]$^{+}$ 100%), 809 ([2M+H]$^{+}$ 51%)

VEAL	100.0	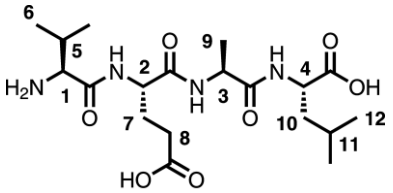 0.94 (dd, J = 18.29, 6.52 Hz, 6H, 12-H), 1.04 (dd, J = 14.29, 6.89 Hz, 6H, 6-H), 1.36 (d, J = 7.11 Hz, 3H, 9-H), 1.61-1.66 (m, 2H, 10-H), 1.73 (tt, J = 13.24, 6.61 Hz, 1H, 11-H), 1.91-2.01 (m, 1H, 5-H), 2.07-2.2 (m, 2H, 7-H), 2.40-2.46 (m, 2H, 8-H), 3.70 (d, J = 5.72 Hz, 1H, 1-H), 4.35-4.49 (m, 3H, 2-H, 3-H, 4-H)	17.8, 18.0, 18.9, 21.8, 23.4, 25.9, 28.4, 31.0, 31.6, 41.7, 50.2, 52.0, 53.9, 59.6, 169.5, 172.5, 174.7, 175.8, 176.5	431 ($[M+H]^+$, 100%), 861 ($[2M+H]^+$, 51%)
VES^{P}L	94.2	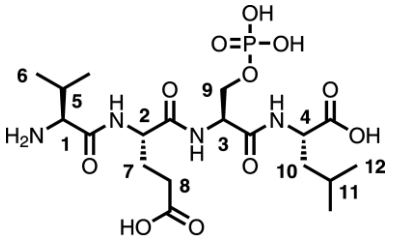 0.94 (dd, J = 16.91, 6.51 Hz, 6H, 12-H), 1.06 (dd, J = 15.97, 6.89 Hz, 6H, 6-H), 1.61-1.67 (m, 2H, 10-H), 1.70-1.78 (m, 1H, 11-H), 1.96-2.07 (m, 1H, 5-H), 2.16-2.29 (m, 2H, 7-H), 2.40-2.51 (m, 2H, 8-H), 3.72 (d, J = 5.54 Hz, 1H, 1-H), 4.11-4.26 (m, 2H, 9-H), 4.39-4.51 (m, 3H, 2-H, 3-H, 4-H)	19.6, 20.6, 23.6, 25.2, 27.3, 29.3, 32.8, 33.8, 43.1, 46.6, 56.1, 57.2, 61.3, 66.7, 172.2, 173.1, 175.7, 180.9, 188.6	561.3 ($[M-H+2NH_4]^+$, 100%), 544.2 ($[M+NH_4]^+$, 92%), 527.2 ($[M+H]^+$, 23%)
VAS^{P}L	87.0	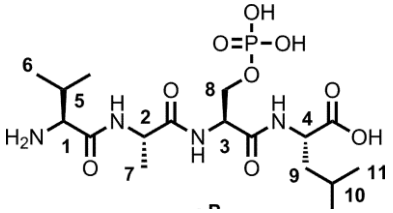 0.95 (dd, J = 11.56, 6.68 Hz, 6H, 11-H), 1.07 (dd, J = 16.45, 6.56 Hz, 6H, 6-H), 1.43 (d, J = 7.15 Hz, 3H, 7-H), 1.59-1.67 (m, 2H, 9-H), 1.68-1.77 (m, 1H, 10-H), 2.14-2.33 (qd, J = 13.29, 6.42 Hz 1H, 5-H), 3.66-3.76 (m, 1H, 1-H), 4.15-4.29 (m, 2H, 8-H), 4.41-4.54 (m, 2H, 2-H, 4-H), 4.56-4.72 (m, 1H, 3-H)	16,5, 18.2, 19.0, 22.0, 23.4, 25.8, 31.4, 51.4, 56.8, 60.0, 65.5, 169.6, 171.7, 174.1	561.3 ($[M-H+2NH_4]^+$, 100%), 544.2 ($[M+NH_4]^+$, 92%), 527.2 ($[M+H]^+$, 23%)

$GES^{P}L$	97.3	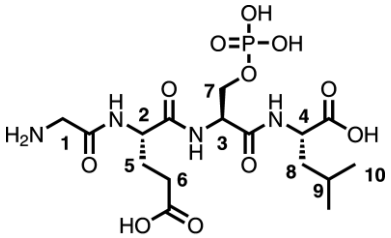 0.94 (ddd, J = 19.30, 6.46, 4.63 Hz, 6H, 10-H), 1.58-1.68 (m, 2H, 8-H), 1.68-1.77 (m, 1H, 9-H), 1.91-2.04 (m, 1H, 5-Ha), 2.10-2.30 (m, 1H, 5-Hb), 2.39-2.50 (m, 2H, 6-H), 3.71 (s, 2H, 1-H), 4.14-4.29 (m, 2H, 7-H), 4.41-4.54 (m, 2H, 2-H, 4-H), 4.62-4.70 (m, 1H, 3-H)	20.8, 22.4, 24.5, 27.3, 40.4, 40.6, 53.6, 54.0, 54.4, 63.8, 89.2, 93.9, 109.8, 161.9	561.3 ($[M-H+2NH_4]^+$, 100%), 544.2 ($[M+NH_4]^+$, 92%), 527.2 ($[M+H]^+$, 23%)

[a] analytical HPLC; [b] 500 MHz, CD_3OD; [c] 75 MHz, CD_3OD; [d] ESI, +10 V

Figures

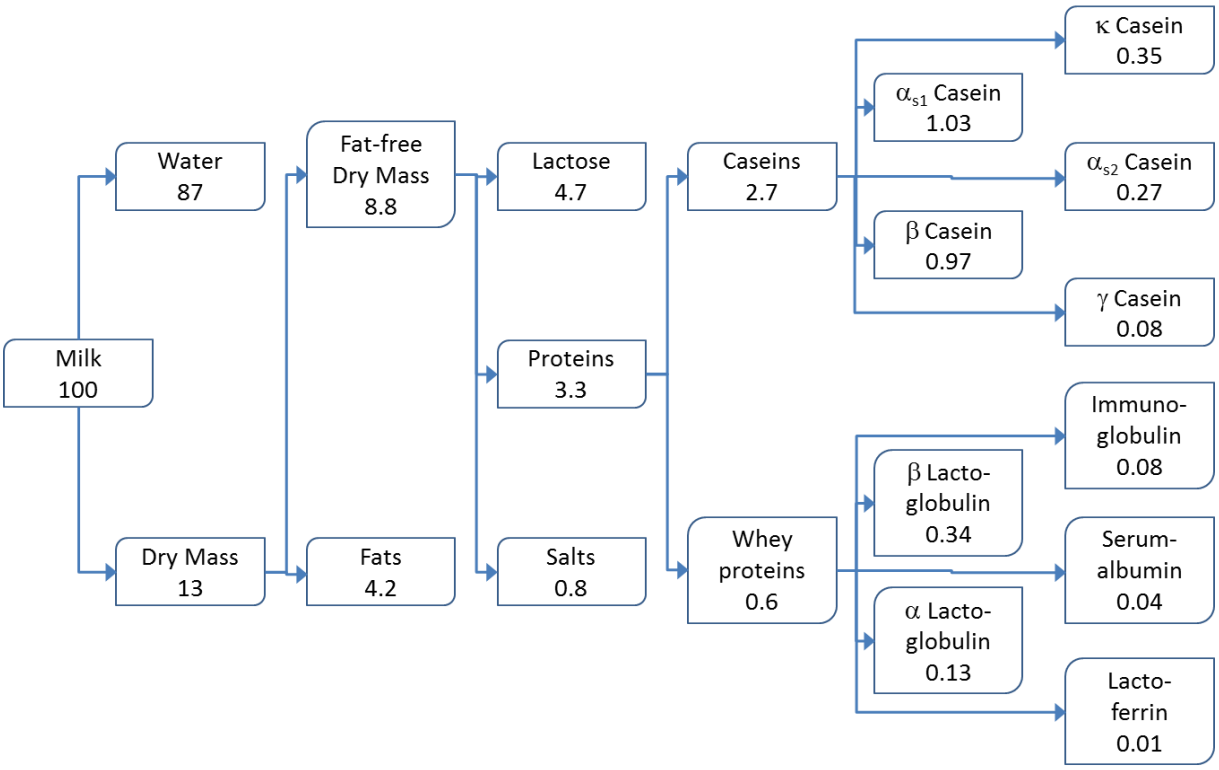

Figure S1. Schematic diagram of the composition of milk (weight %).[1]

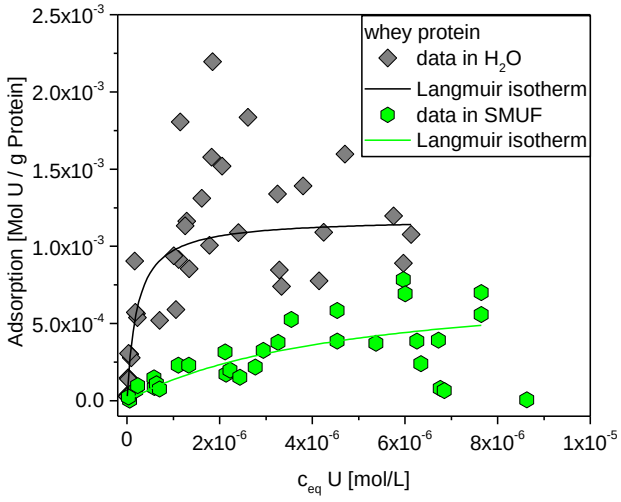

Figure S2. Experimental data and fitted Langmuir isotherm of uranium(VI) adsorption onto whey protein in water (black) and in SMUF solution (green); pH 4.6.

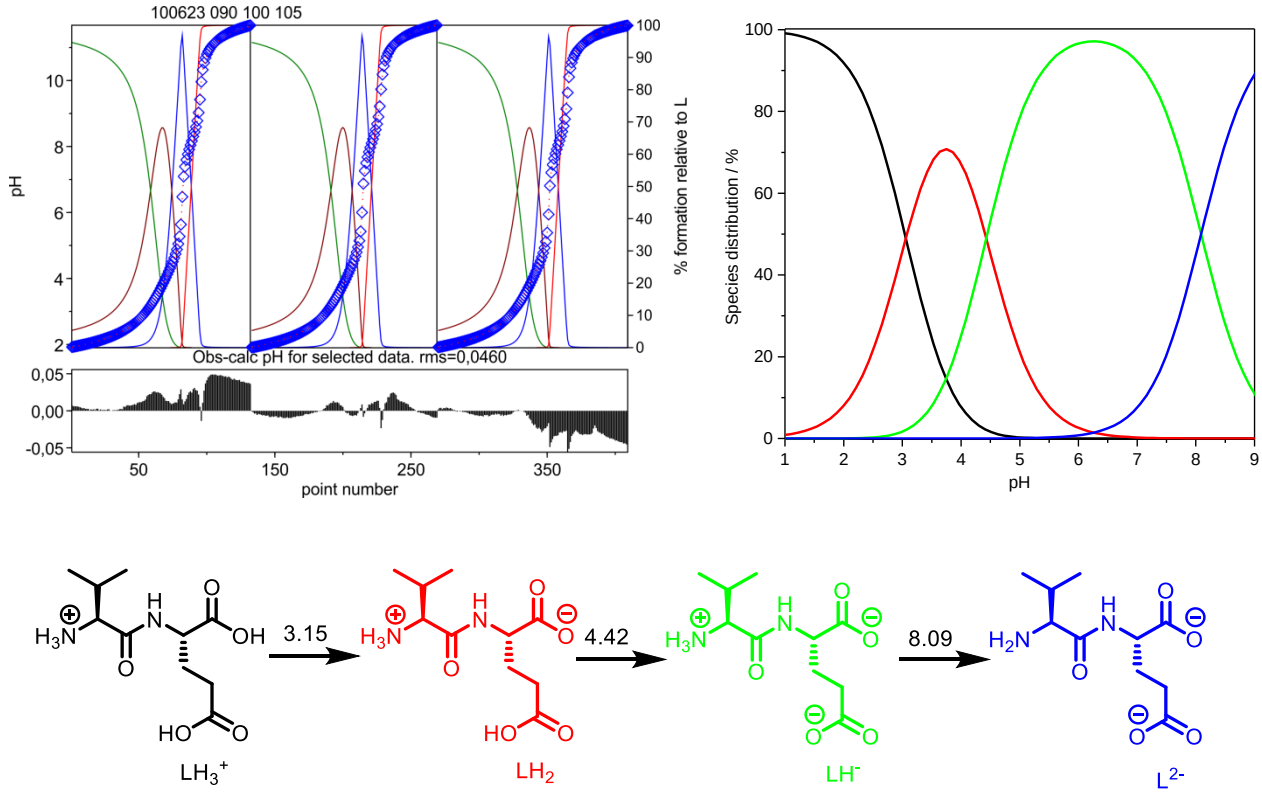

Figure S3. Potentiometric titration curves together with fits and residuals, speciation and respective species of VE in dependence on pH at a peptide concentration of $3 \cdot 10^{-3}$ M (I = 0.1 M).

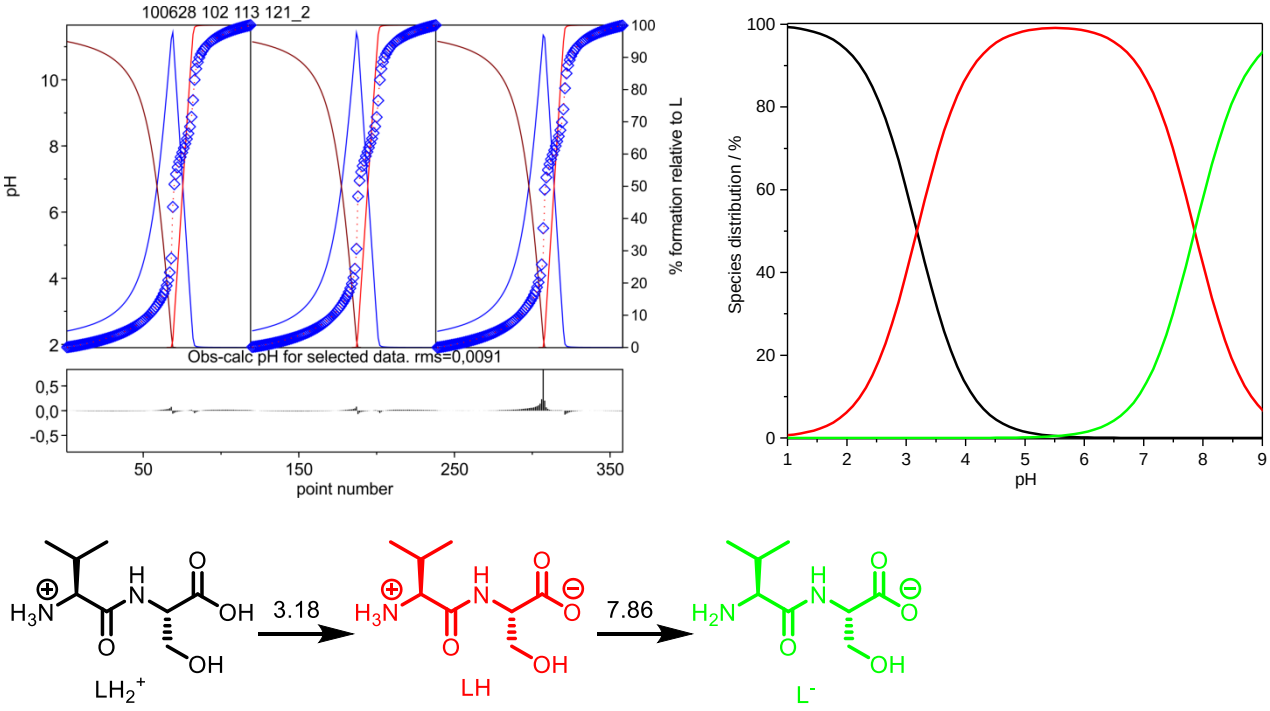

Figure S4. Potentiometric titration curves together with fits and residuals, speciation and respective species of VS in dependence on pH at a peptide concentration of $3 \cdot 10^{-3}$ M (I = 0.1 M).

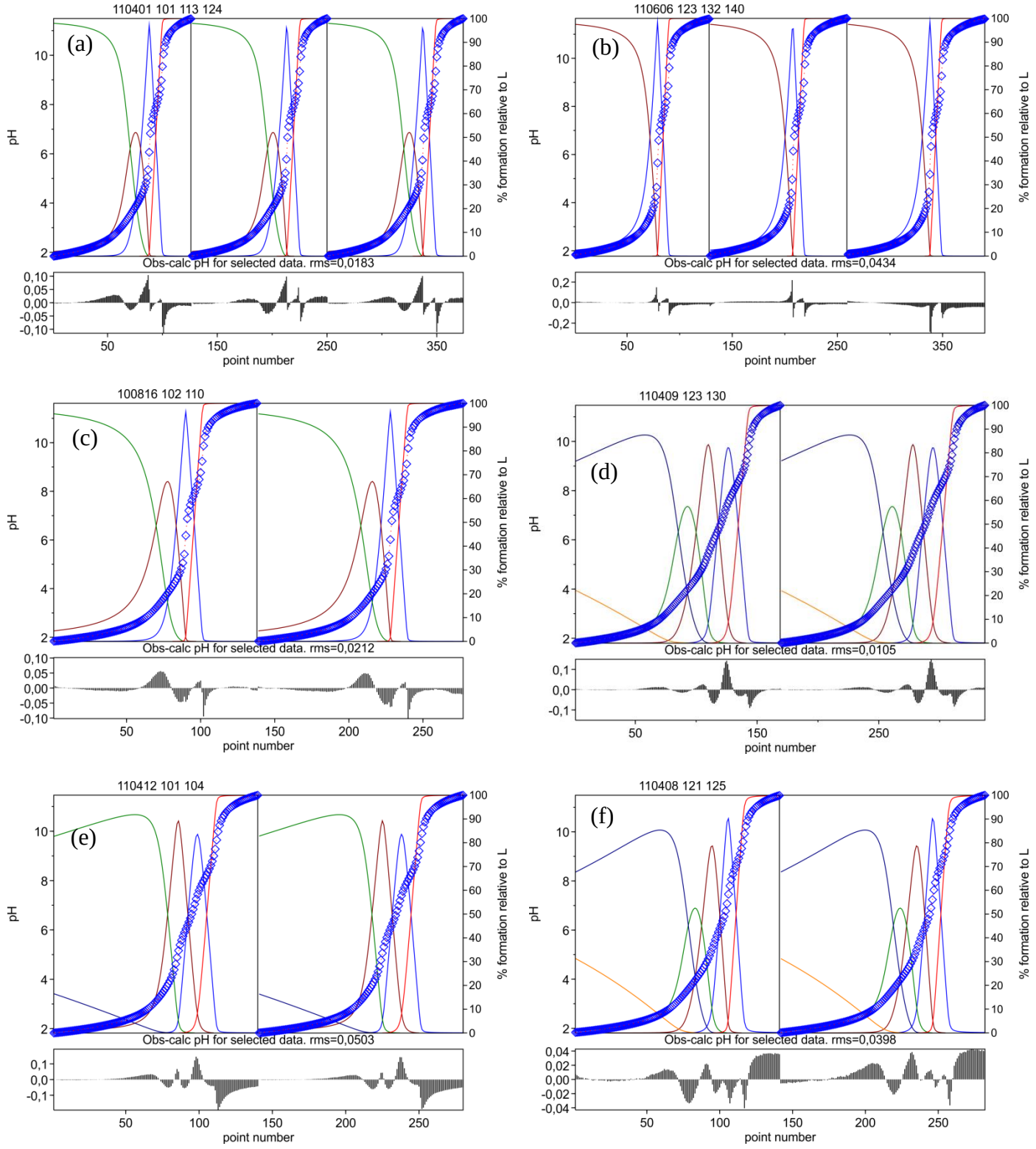

Figure S5. Potentiometric titration curves together with fits and residuals of the dephosphorylated tetrapeptides VESL (a), VASL (b), VEAL (c), VES^{P}L (d), VAS^{P}L (e) and GES^{P}L (f) in dependence on pH at a peptide concentration of $3 \cdot 10^{-3}$ M (I = 0.1 M).

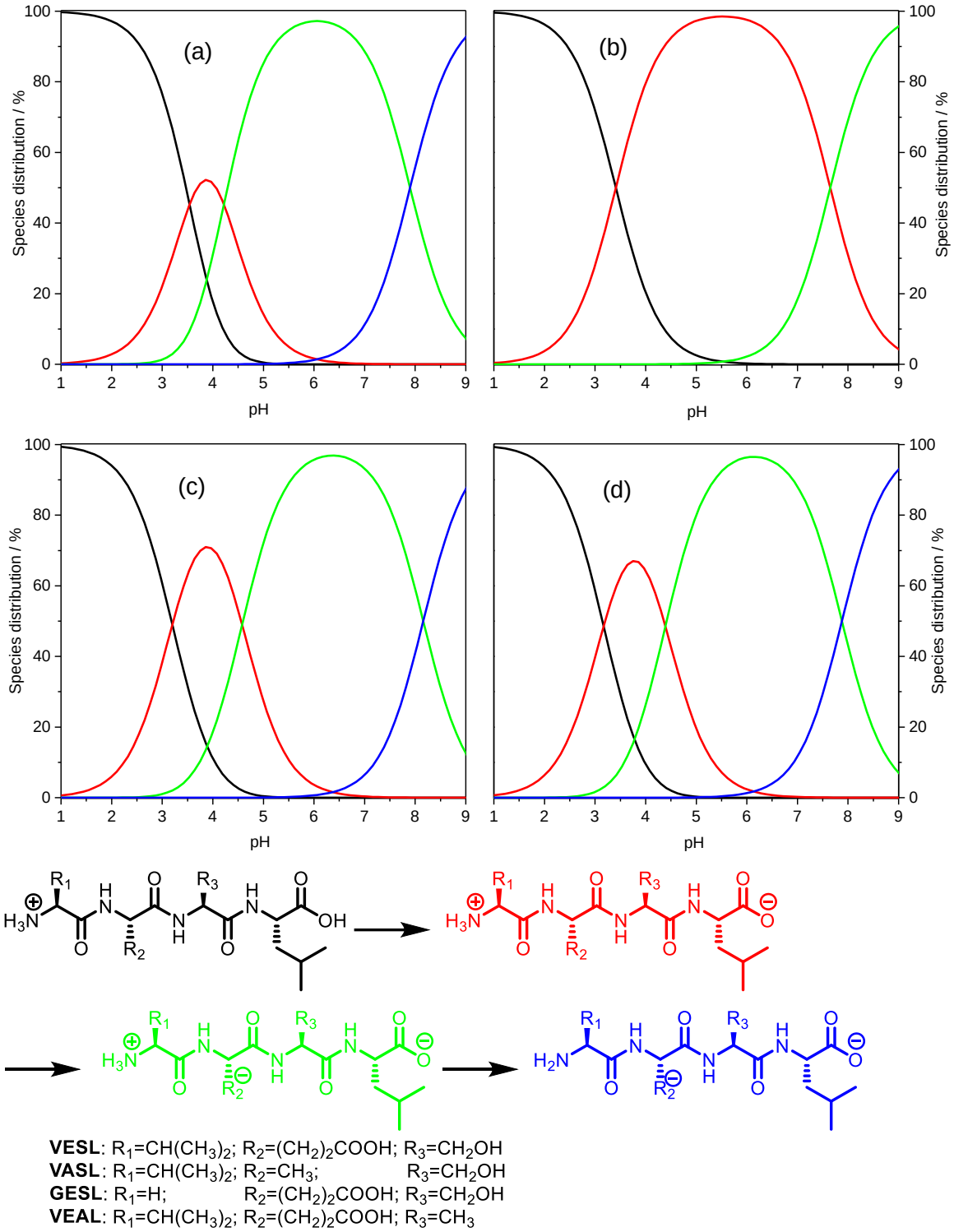

Figure S6. Speciation and respective species of the dephosphorylated tetrapeptides VESL (a), VASL (b), GESL (c) and VEAL (d) in dependence on pH at a peptide concentration of $3 \cdot 10^{-3}$ M (I = 0.1 M).

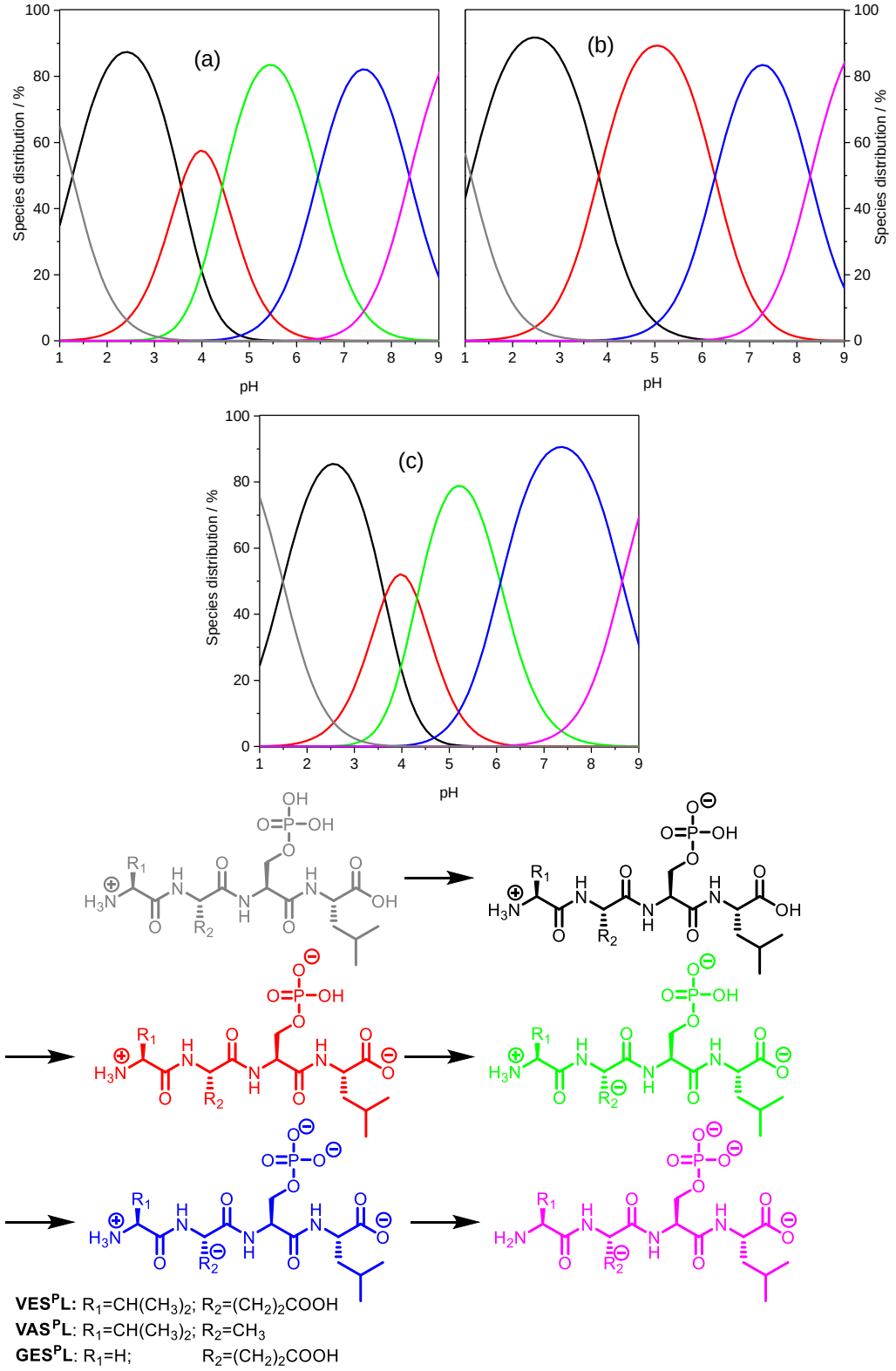

Figure S7. Speciation and respective species of the phosphorylated tetrapeptides VES^{P}L (a), VAS^{P}L (b) and GES^{P}L (c) in dependence on pH at a peptide concentration of $3 \cdot 10^{-3}$ M (I = 0.1 M).

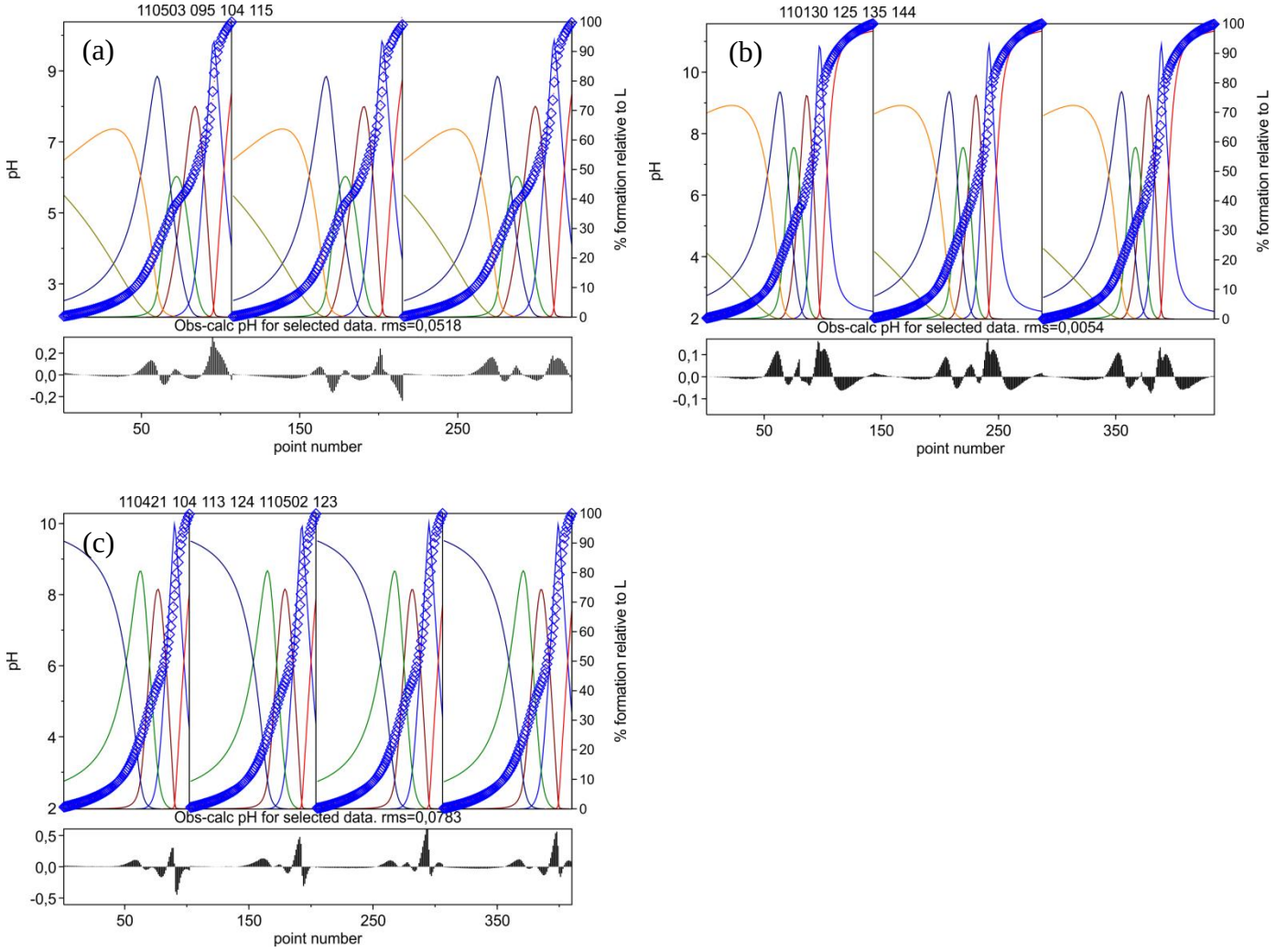

Figure S8. Potentiometric titration curves together with fits and residuals of the proteins "acid casein" (a), β-casein (b) and dephosphorylated "acid casein" (c) in dependence on pH at a protein concentration of $3 \cdot 10^{-4}$ M (I = 0.1 M).

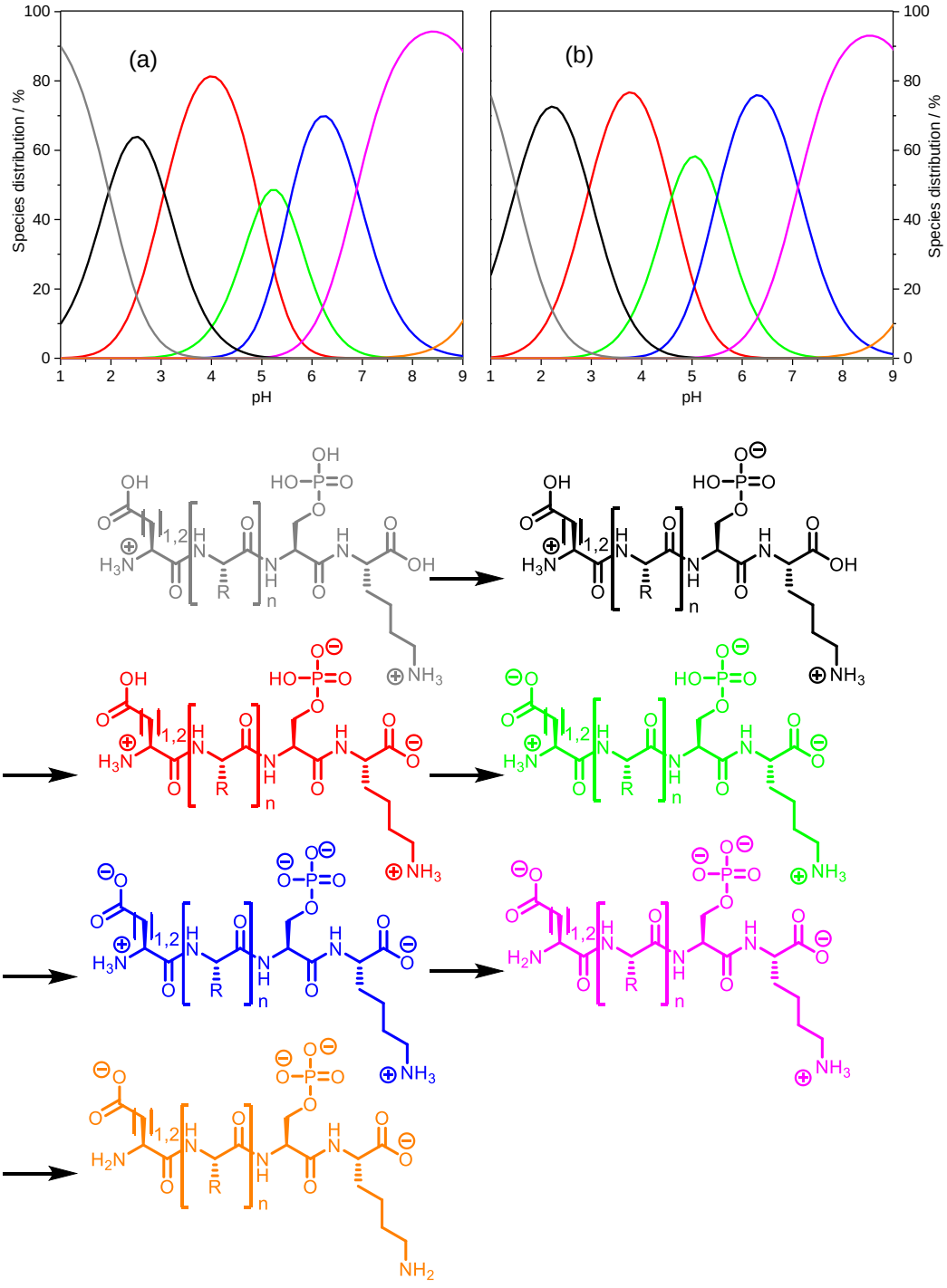

Figure S9. Speciation and respective species of the proteins "acid casein" (a) and β-casein (b) in dependence on pH at a protein concentration of $3 \cdot 10^{-4}$ M (I = 0.1 M).

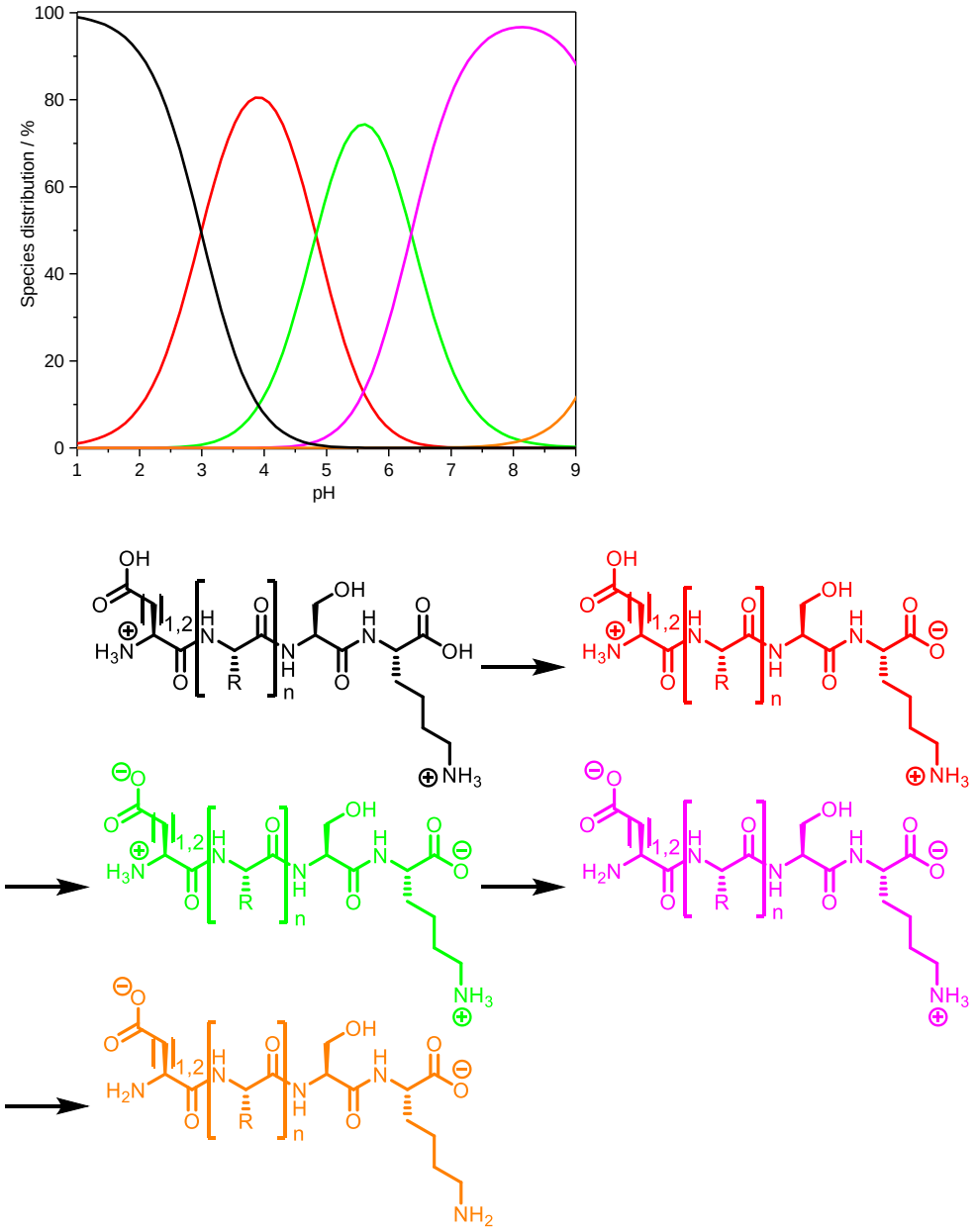

Figure S10. Speciation and respective species of the dephosphorylated “acid casein” in dependence on pH at a protein concentration of $3 \cdot 10^{-4}$ M (I = 0.1 M).

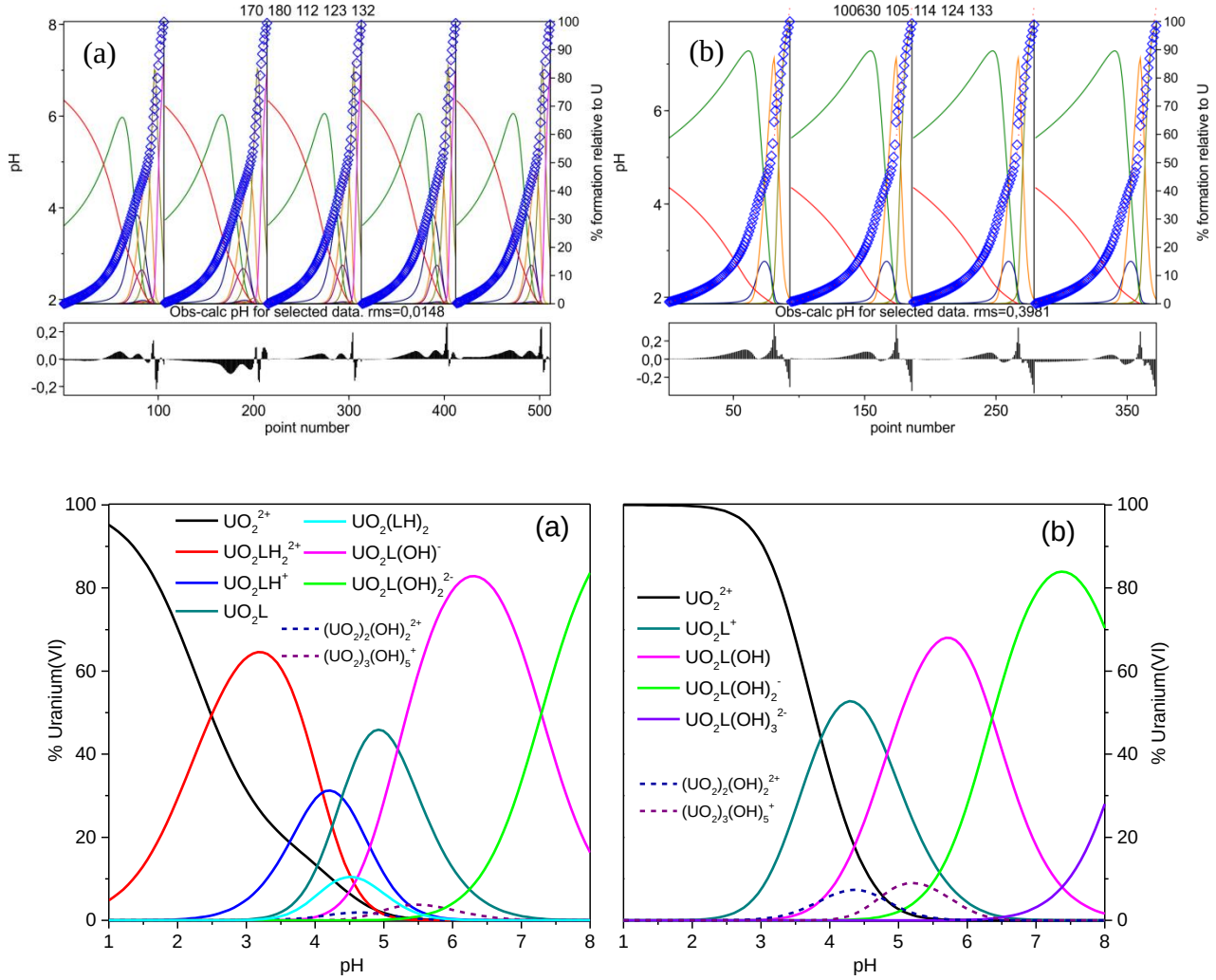

Figure S11. Potentiometric titration curves together with fits and residuals (top) and speciation of uranium(VI) (bottom) with VE (a) and VS (b) in dependence on pH at a uranyl concentration of $1.5 \cdot 10^{-3}$ M and ligand concentration of $3.0 \cdot 10^{-3}$ M (I = 0.1 M).

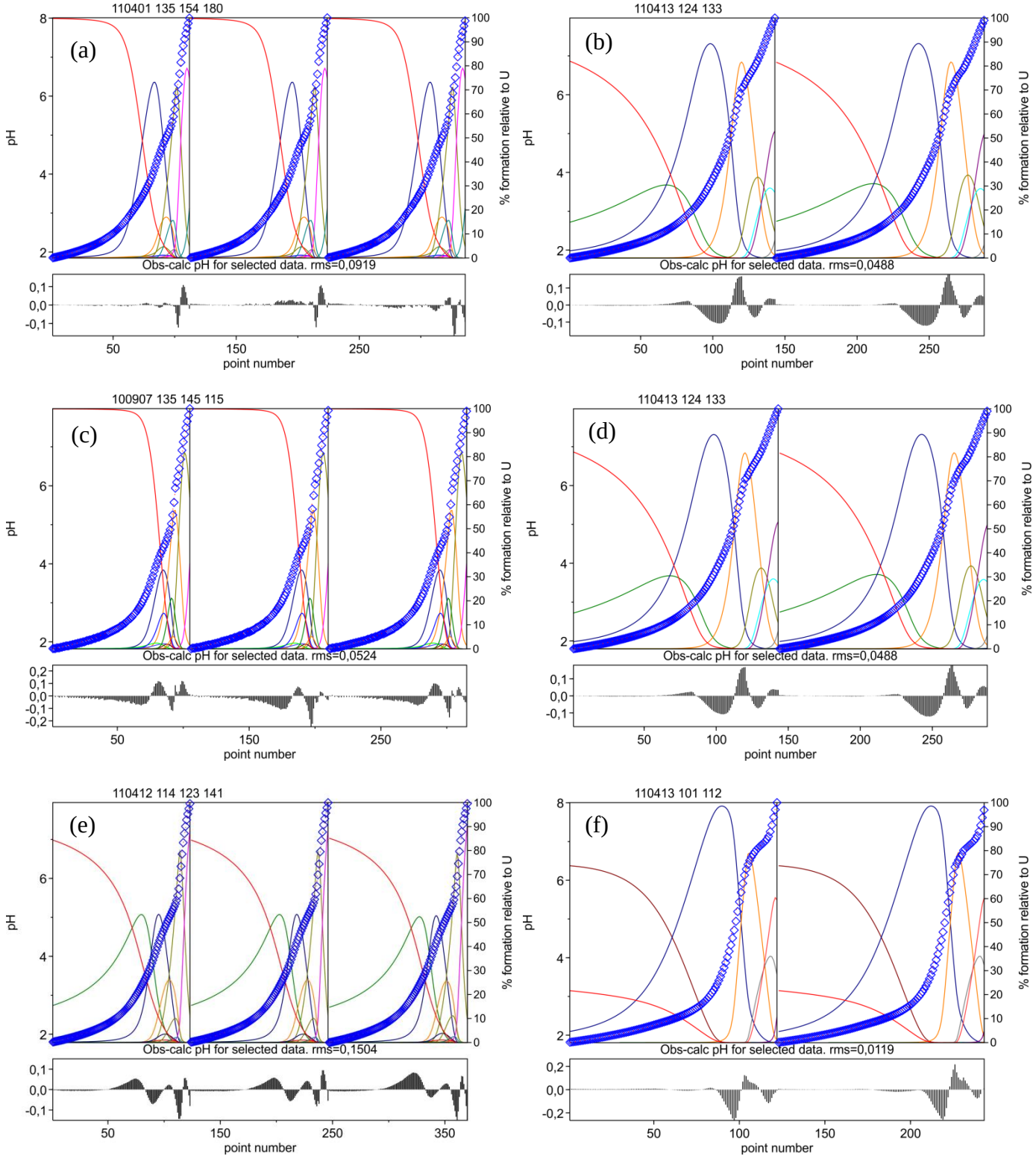

Figure S12. Potentiometric titration curves together with fits and residuals of uranium(VI) with VESL (a), VES^{P}L (b), VASL (c), VAS^{P}L (d), GESL (e), and GES^{P}L (f) in dependence on pH at a uranyl concentration of $1.5 \cdot 10^{-3}$ M and ligand concentration of $3.0 \cdot 10^{-3}$ M (I = 0.1 M).

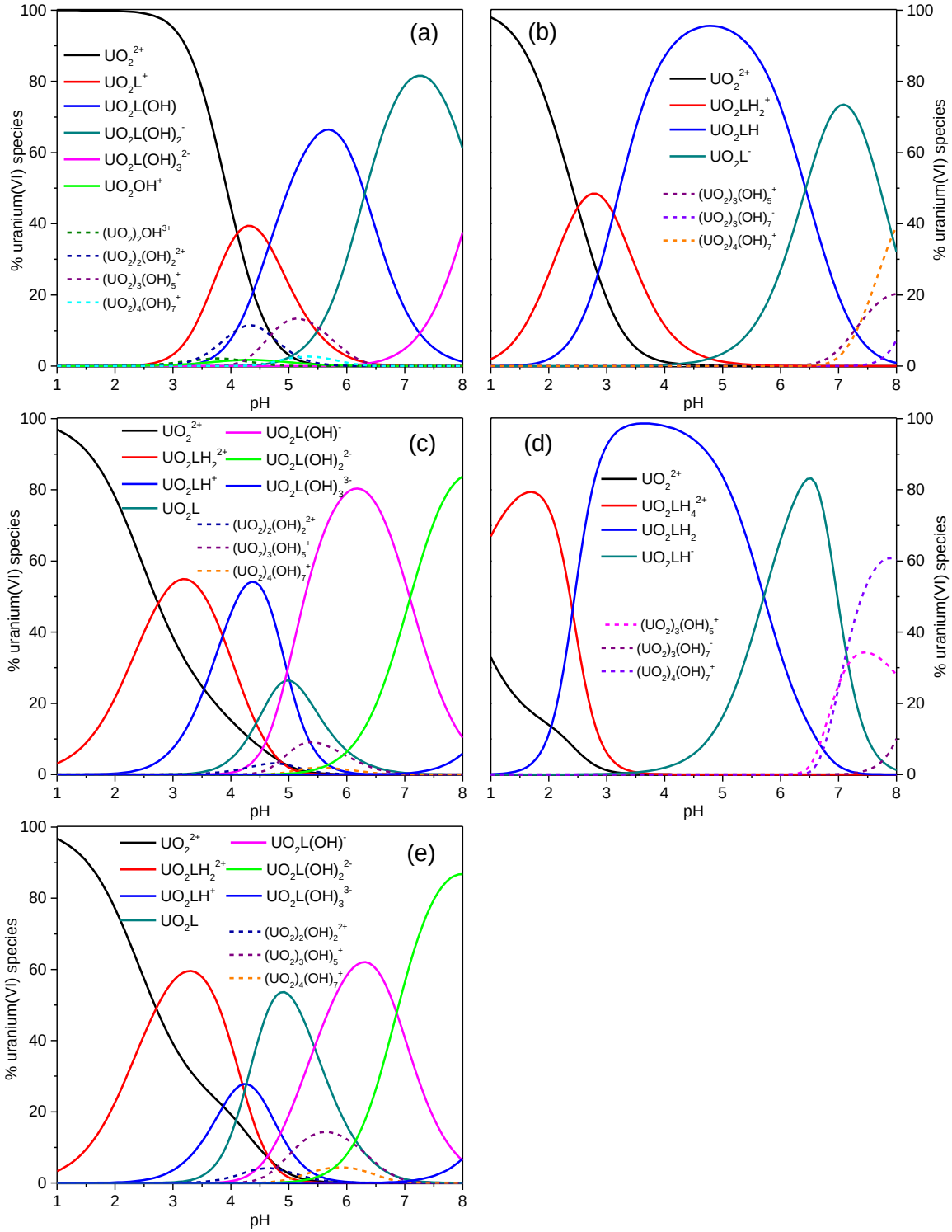

Figure S13. Speciation of uranium(VI) with VASL (a), VAS^{P}L (b), GESL (c), GES^{P}L (d) and VEAL (e) in dependence on pH at a uranyl concentration of $1.5 \cdot 10^{-3}$ M and ligand concentration of $3.0 \cdot 10^{-3}$ M (I = 0.1 M).

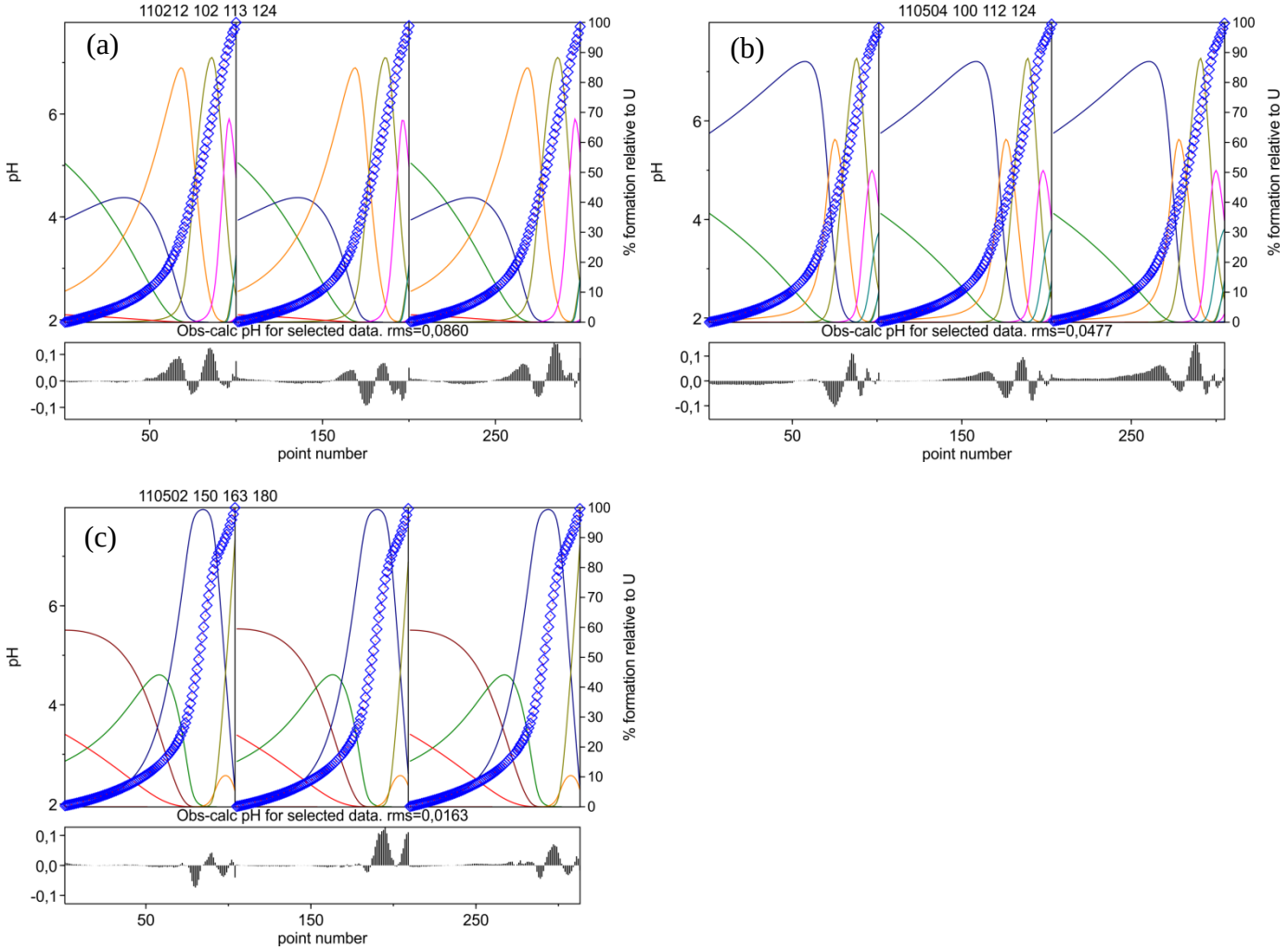

Figure S14. Potentiometric titration curves together with fits and residuals of uranium(VI) with ß-casein (a), "acid casein" (b) and dephosphorylated "acid casein" (c) in dependence on pH at a uranyl concentration of $1.0 \cdot 10^{-3}$ M and ligand concentration of $3.0 \cdot 10^{-4}$ M (I = 0.1 M $NaClO_4$).

References

1. Schlimme, E.; Buchheim, W., *Milch und ihre Inhaltsstoffe – Chemische und physikalische Eigenschaften*. 2 ed.; Verlag Th. Mann: Gelsenkirchen (in German), 1999.
2. Aoki, T.; Yamada, N.; Tomita, I.; Kako, Y.; Imamura, T. Caseins are cross-linked through their ester phosphate groups by colloidal calcium-phosphate. *Biochim. Biophys. Acta* **1987,** *911*, 238-243.
3. Heine, K. B. U(VI) binding onto milk proteins and model peptides. PhD thesis,Technische Universität Dresden, Germany (in German), 2016.
4. Farrell, H. M.; Malin, E. L.; Brown, E. M.; Qi, P. X. Casein micelle structure: What can be learned from milk synthesis and structural biology? *Curr. Opin. Colloid Interface Sci.* **2006,** *11*, 135-147.
5. Jenness, R.; Koops, J. Preparation and properties of a salt solution which simulates milk ultrafiltrate. *Neth. Milk Dairy J.* **1962,** *16*, 153-164.
6. Berthon, G. Critical evalution of the stability-constants of metal-complexes of amino-acids with polar side-chains. *Pure Appl. Chem.* **1995,** *67*, 1117-1240.
7. Yamauchi, O.; Odani, A.; Masuda, H. Weak interactions in metal complexes of amino acids with a phosphorylated side chain. Conversion of aromatic ring stacking to electrostatic bonding by tyrosine phosphorylation. *Inorg. Chim. Acta* **1992,** *198-200*, 749-61.
8. Guillaumont, R.; Fanghänel, T.; Fuger, J.; Grenthe, I.; Neck, V.; Palmer, D. A.; Rand, M. H., *Update on the Chemical Thermodynamics of Uranium, Neptunium, Plutonium, Americium and Technetium.* Elsevier: Amsterdam, 2003.